Theses and Dissertations

12-2015

High-Frequency Transformer Design for Solid-State Transformers in Electric Power Distribution Systems

Roderick Javier Garcia Montoya
University of Arkansas, Fayetteville

High-Frequency Transformer Design for Solid-State Transformers in Electric Power Distribution
Systems

A thesis submitted in partial fulfillment
of the requirements for the degree of
Master of Science in Electrical Engineering

by

Roderick Javier Garcia Montoya
Universidad Tecnológica de Panamá
Bachelor of Science in Electromechanical Engineering, 2011

December 2015
University of Arkansas

This thesis is approved for recommendation to the Graduate Council.

_____
Dr. Juan Carlos Balda
Thesis Director

_____   _____
Dr. Simon Ang   Dr. Roy McCann
Committee Member   Committee Member

ABSTRACT

The objective of this thesis is to present a high- or medium-frequency transformer design methodology for Solid-State Transformer (SST) applications. SSTs have been proposed as a replacement of the traditional 50/60 Hz transformer in applications demanding high-power density. Moreover, due to the high penetration of distributed generation, DC grids, energy storage systems, and sensitive loads, SSTs have been considered as an enabling technology for envisioned future energy systems. These applications demand additional functionalities that may not be achieved with traditional transformers. For example, active power flow control, harmonic suppression, voltage regulation, voltage sag compensation, and reduced size and volume.

In this thesis, SST topologies are evaluated in order to determine their impact upon the transformer design. In addition, design considerations for core and wire selections, isolation requirements, and different transformer structures are investigated. As a result, the proposed transformer design methodology accounts for leakage inductance requirements for optimal power transfer, high-frequency effects in the transformer core and windings, and a flux density optimization to maximize transformer's efficiency. The design procedure has been implemented in MATLAB$^®$ as an interactive tool for designing high-frequency transformers.

ACKNOWLEDGEMENTS

DEDICATION

Esta tesis va dedicada a Dios quien ha sido siempre mi guía y fortaleza. A mis padres, Oderay y Roderick, por el amor e incondicional apoyo que me han brindado. Sus consejos y ejemplos de perseverancia me han motivado durante toda mi vida.

También, a mi hermana Zurisadai y mi hermano Alfredo por creer en mí y estar siempre presentes. A mis sobrinos quienes son parte de mi motivación y felicidad. A mi familia en general y amigos por incentivarme a nunca rendirme. En particular, a mi tía Nubia Montoya por motivarme y brindarme su apoyo.

Finalmente dedico esta tesis a todas las personas que Dios puso en mi camino durante mis años de estudio en los Estados Unidos. En especial a Bianca Montes, Orla Engstrom, Rebecca Garrett y Tyler Coopland por abrirme las puertas de sus hogares y hacerme sentir como en casa.

TABLE OF CONTENTS

LIST OF FIGURES

LIST OF TABLES

CHAPTER 1

INTRODUCTION

1.1 Motivations for this Research

A transformer is a device that can transfer energy by means of electromagnetic induction [1], [2]. Its basic structure consists of a magnetic core and two independent windings (primary and secondary). The transformer operation is described by Ampere's law and Faraday's law. The former states that a current flowing through a conductor produces a magnetic field around the conductor. The latter, Faraday's law, states that a changing magnetic field flowing in a closed circuit can induce a voltage across a conductor which is proportional to the rate of change of the magnetic flux. Hence, an alternating current flowing through the transformer primary winding produces a changing magnetic field that flows through the magnetic core and induces a voltage across the secondary winding.

Therefore, transformers are used in applications where it is necessary to step-down or step-up a voltage from one level to another one and create an electric isolation between two circuits. For instance, they are widely used in electric power grids, which are constituted by four main systems as depicted in Fig. 1.1 [1]: power generation, transmission, distribution, and customers. In power generation the voltage is stepped up to a transmission level (e.g. 345, 230, 138, 115 kV) to transport electric energy more efficiently [1], [2]. From the transmission level, the voltage is reduced to a level suitable for power distribution (e.g. 34.5Y/19.92, 13.2Y/7.62, 12.47Y/7.2, 4.16Y/2.4 kV) [1], [2]. Finally, depending on the type of service (three phases or single phase), the voltage is again stepped down from the customer receiving end to a usable voltage (e.g. 480Y/277, 208Y/120, 240/120 V) [2].
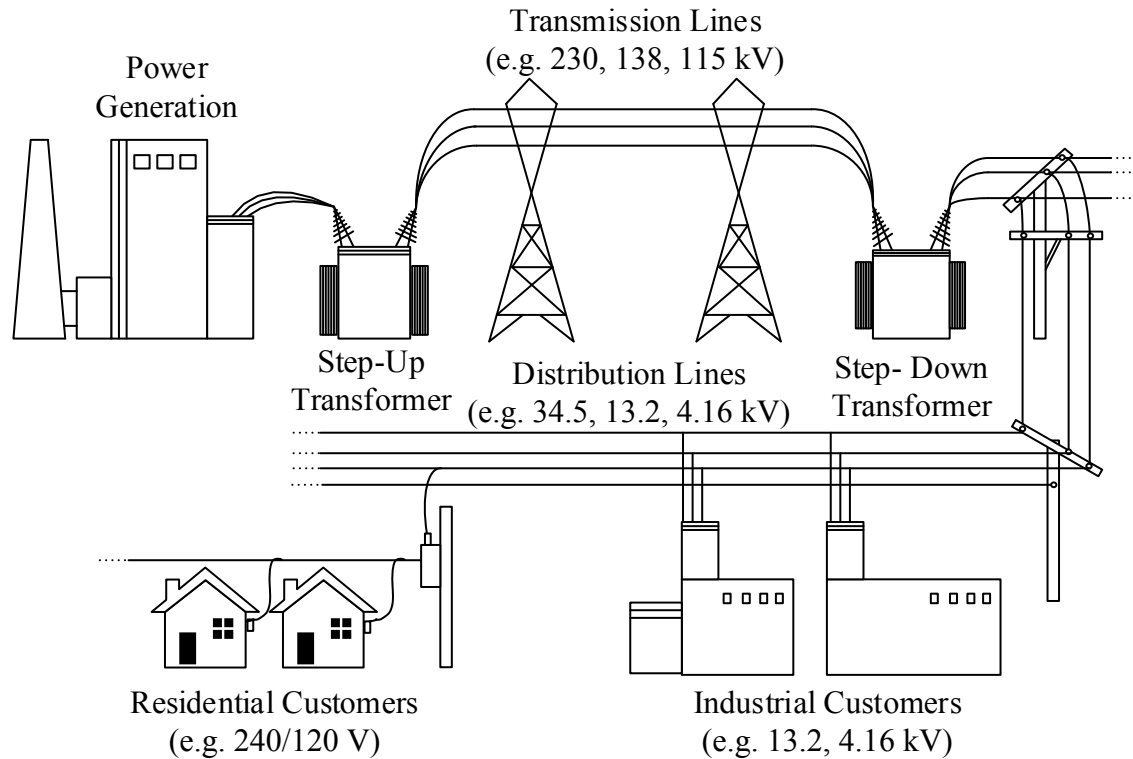
Fig. 1.1. Generic electric power system

In those applications, traditional transformers are operated at line frequency (50 Hz/60 Hz) and can achieve efficiencies as high as ~ 99% [2], [3].

1.1.1 Solid-State Transformer Functionalities

The traditional transformer performs its function very efficiently. However, it is envisioned that future energy systems will demand additional functionalities (besides stepping up/down voltages) that are not achievable with the traditional 50/60 Hz transformer [3], [4]. Examples of these functionalities are the following:

- Active power flow control to achieve reactive power compensation and energy exchange between energy storage elements and the distribution system [4], [5].

2

- Regulated low-voltage (LV) DC link to facilitate the integration of energy storage systems, renewable energy sources, and DC loads such as DC buildings and future DC grids [3]-[5].

- Voltage sag compensation, fault current limiting, and power quality improvement demanded by the deployment of sensitive loads (e.g., server farms) [4], [5].

- Volume and weight reductions which are critical in applications characterized by space limitations [6]; for example, electric locomotives.

The above mentioned functionalities can be achieved by implementing the concept of Solid-State Transformer (SST), also called power-electronic transformer or intelligent universal transformer. The SST is a power electronic interface which combines power converters, high-frequency (HF) or medium-frequency (MF) transformers, and control circuitry [3]-[9]. The primary concept is to replace the traditional 50/60 Hz transformer with a HF or MF transformer which enables an important reduction in volume and weight; therefore, SSTs have been proposed for applications such as train traction, charging systems of electric vehicles, off-shore wind farms, and tidal power plants [7], [9]. More recently, due to continuous advancements on power semiconductor devices and more efficient converter topologies, more research has been devoted to the implementation of SSTs in distribution systems and smart grids [3]-[5].

1.1.2 Generic SST Configuration

A generic configuration to realize a SST is shown in Fig. 1.2 [7]-[9]. This configuration consists of three stages: an active-front-end rectifier stage (AC-DC), a dual-active bridge (DAB) stage (DC-DC) with a HF or MF transformer, and a back-end inverter stage (DC-AC) [10], [11]. The rectifier stage enables the high-voltage (HV) DC link and input current control.

3
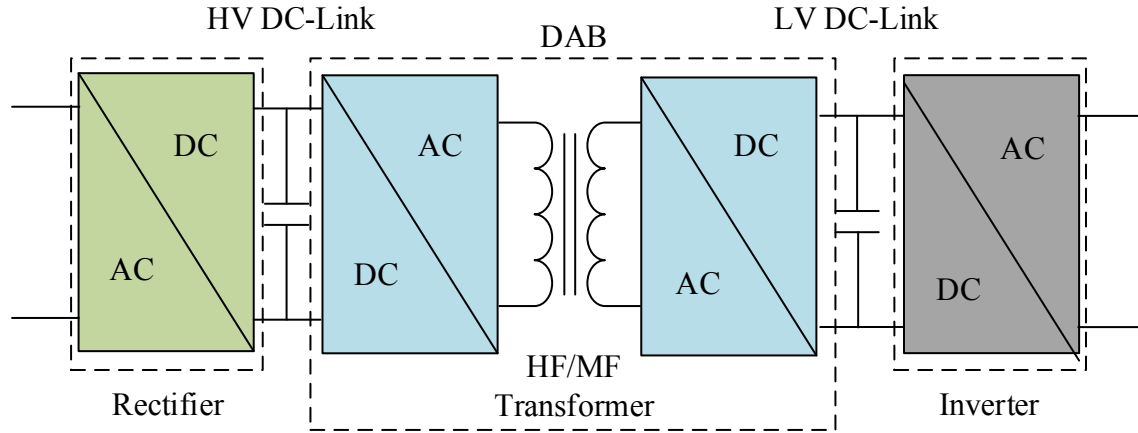
Fig. 1.2. Three-stage SST configuration

The DAB stage regulates the LV DC link, steps up/down a voltage from one level to another one, and allows power flow control. The transformer leakage inductance is used to storage and transfer energy. Lastly, the inverter stage changes the voltage back to 50/60 Hz to connect the AC loads.

1.1.3   Challenges in the High-Frequency Transformer Design

The HF/MF transformer in the DC-DC stage performs the same function as the traditional 50/60 Hz transformer which is to enable voltage transformation and provide electrical isolation between HV and LV sides. However, the operation at high voltages and frequencies creates new challenges in the transformer design [12]-[15]:

- High-frequency operation leads to higher core loss and temperature, thus the selection of a magnetic material with high saturation flux density, low specific loss, and high operation temperature is critical to achieve high efficiency and power density [5], [7], [14], [16].

- Since reduced volume and weight is a desired feature, isolation requirements and thermal management must be carefully considered [13], [14].

4

- Skin and proximity effects in the windings are significantly increased when compared with the operation at 50/60 Hz; therefore, special attention must be paid to the wire selection [14], [17].

- The core and winding arrangements must be selected based on the thermal considerations and the leakage inductance requirement for maximum power transfer in the DC-DC stage [12]-[14].

1.2 Thesis Objectives

The main objective of this thesis is to develop a single-phase HF/MF transformer design procedure that considers the requirements for optimal power transfer imposed by SST topologies for distribution systems while, simultaneously, taking into account the HF effects in the core and windings, as well as the calculation of an optimum operating flux density to maximize transformer's efficiency. The main objective will be accomplished through the following specific objectives:

- Evaluate different SST topologies suitable for distribution systems.

- Analyze the requirements that SST topologies impose on the transformer design.

- Evaluate the design tradeoffs between cost, efficiency, and volume which involves a proper core material selection and operating conditions.

- Study design considerations to minimize the HF effects in transformers core and windings.

- Investigate high-voltage isolation considerations for the implementation of SST in distribution systems.

- Study the flux density optimization to maximize transformer's efficiency and power density.

1.3 Case Study

A case study rated 1.8 MW (600 kW per phase) is considered throughout this thesis for evaluation purposes. The HV side is connected to a distribution system whose voltage is 7.2 kV AC (rms per phase) and the LV DC bus is rated at 400 V DC for interconnection of DC loads such as DC buildings. Insulated gate bipolar transistors (IGBTs) are selected as the switching devices for the power converters; in particular, 6.5kV IGBTs are considered for the HV side and 1.2kV IGBTs for the LV side. The selected operating frequency of the HF transformer is 3 kHz due to the frequency capability of the selected switching devices when considering soft-switching operation [13], [19]. Input-series-output-parallel connection of multiple SST modules is considered in order to achieve the required current and voltage ratings, as shown in Fig 1.3 [3]-[6]. A summary of the case-study specifications is given in Table 1.1.

The three-phase system can be interconnected with single-phase based SSTs in each phase or with a three-phase based SST arrangement. The three-phase approach has advantages over the single-phase approach in high-power applications, such as a smaller transformer area product, lower rms currents through the DC link capacitors, and lower turn-off switching loss [10], [18]. However, the single-phase approach is still widely utilized for practical purposes and analysis simplification, thus this approach is chosen for the considered case study.

6

1.4 Thesis Organization

This thesis is organized as follows: a review of SST topologies will be presented in Chapter 2 in order to study their impact upon the HF/MF transformer design. Considerations for core and wire selections are addressed in Chapter 3, which also includes an analysis of the design tradeoffs and a core loss comparison of different magnetic materials. The proposed HF/MF transformer design methodology is presented in Chapter 4, which considers flux density optimization for a minimum loss design, as well as leakage inductance requirements of SST topologies. Transformer design examples and fabrication of scaled-down prototypes to test the validity of the proposed design approach are also presented in this chapter. Finally, conclusions and recommendations for future work will be given in Chapter 5.
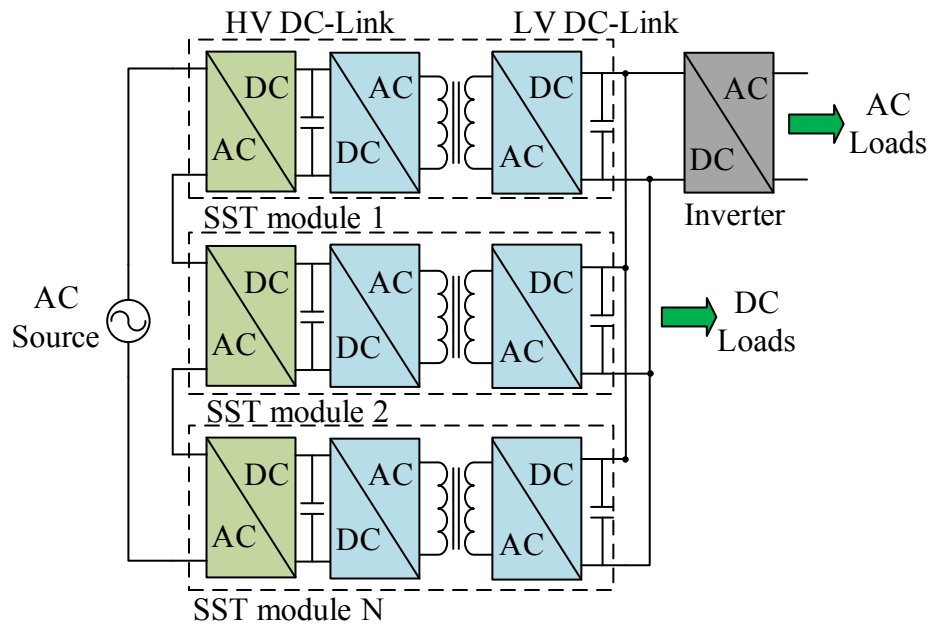
Fig. 1.3. Modular single-phase SST arrangement

Table 1.1. Single-phase case study specifications

Output Power	600 kW
Input Voltage	7.2 kV AC rms
Output Voltage	400 V DC
Transformer Operating Frequency	3 kHz
HV Switching Device	6.5 kV IGBT
LV Switching Device	1.2 kV IGBT

1.5 Publications Resulting from Thesis Work

- R. J. Garcia Montoya, A. Mallela, J. C. Balda, "An evaluation of selected solid-state transformer topologies for electric distribution systems," in *Proceedings of the IEEE 30th Applied Power Electronics Conference and Exposition*, APEC 2015, pp. 1022-1029, March 2015.

- R. Garcia, A. Escobar-Mejía, K. George, J. C. Balda, "Loss comparison of selected core magnetic materials operating at medium and high frequencies and different excitation voltages," in *Proceedings of the IEEE 5th International Symposium on Power Electronics for Distributed Generation Systems*, PEDG 2014, pp. 1-6, June 2014.

1.6 References

[1]   T. Gonen, <u>Electric Power Distribution System Engineering</u>, Second Edition. Boca Raton, FL: CRC Press Taylor & Taylor Group, 2008.

[2]   L. M. Faulkenberry and W. Coffer, <u>Electrical Power Distribution and Transmission</u>. Englewood Cliffs, NJ: Prentince Hall, 1996.

[3]   X. She, R. Burgos, G. Wang, F. Wang, A.Q. Huang, "Review of solid state transformer in the distribution system: From components to field application," in *Proceedings of the IEEE Energy Conversion Congress and Exposition*, ECCE 2012, pp. 4077–4084, Sept., 2012.

[4]   J. W. Kolar, G. Ortiz, "Solid-state-transformers: Key components of future traction and smart grid systems," in *Proceedings of the International Power Electronics Conference*, IPEC 2014, Japan, May 18-24, 2014.

[5]   S. Xu, Y. Xunwei, F. Wang, A. Q. Haung, " Design and demonstration of 3.6 kV-120 V/10 kVA solid-state transformer for smart grid application," *IEEE Transactions on Power Electronics*, vol. 29, no. 8, pp. 3982-3988, Aug 2014.

[6]   D. Dujic, F. Kieferndorf, F. Canales, U. Drofenik, "Power electronic traction transformer technology," in *Proceedings of the 7th IEEE International Power Electronics and Motion Control Conference*, IPEMC 2012, China, pp. 636–642, June 2-5, 2012.

[7]   X. She, A. Q. Huang, R. Burgos, "Review of solid-state transformers technologies and their application in power distribution systems," *IEEE Journal of Emerging and Selected Topics in Power Electronics*, vol. 1, no. 3, pp. 186-198, Sept. 2013.

[8]   S. Falcones, X. Mao, R. Ayyanar, "Topology Comparison for Solid State Transformer Implementation," IEEE Power and Energy Society General Meeting, pp. 1-8, July 2010.

[9]   J. W. Kolar, "Intelligent solid state transformers (SSTs) a key building block of future smart grid systems," [Online]. Available: http://www.pes.ee.ethz.ch/uploads/tx_ethpublications/CPSSC_2011_China_MEGACube_as_presented.pdf

[10] R.W.A.A. De Doncker, D.M. Divan, M.H. Kheraluwala, "A three-phase soft-switched high-power-density DC/DC converter for high-power applications," *IEEE Transactions on Industry Applications*, vol. 27, no. 1, pp. 63-73, Jan./Feb. 1991.

[11] B. Zhao, S. Qiang, W. Liu, Y. Sun, "Overview of Dual-Active-Bridge isolated bidirectional DC-DC converter for high-frequency-link power-conversion system," *IEEE Transactions on Power Electronics*, vol. 29, no. 8, pp. 4091-4106, August 2014.

[12] K. D. Hoang, J. Wang, "Design optimization of high-frequency transformer for dual active bridge dc-dc converter," *XXth International Conference Electrical Machines* (ICEM), pp. 2311-2317, September 2012.

[13] Y. Du, S. Baek, S. Bhattacharya, A. Q. Huang, "High-voltage high-frequency transformer design for a 7.2kV to 120V/240V 20kVA solid state transformer," in *Proceedings of the 36th*

IEEE Industrial Electronics Society Conference, IECON 2010, pp. 493-498, November 2010.

[14] G. Ortiz, J. Biela, J. W. Kolar, "Optimized design of medium frequency transformers with high isolation requirements," in *Proceedings of the 36th IEEE Industrial Electronics Society Conference*, IECON 2010, pp. 631-638, November 2010.

[15] G. Ortiz, M. Leibl, J.W. Kolar, O. Apeldoorn, "Medium frequency transformers for solid-state-transformer applications — Design and experimental verification," in *Proceedings of the 10th IEEE International Conference on Power Electronics and Drive Systems*, PEDS 2013, pp. 1285–1290, April 2013.

[16] R. Garcia, A. Escobar-Mejia, K. George, J.C. Balda, "Loss comparison of selected core magnetic materials operating at medium and high frequencies and different excitation voltages," in *Proceedings of the 5th International Symposium on Power Electronics for Distributed Generation Systems*, PEDG 2014, pp. 1-6, June 2014.

[17] W.G. Hurley, W. H. Wöfle, J. G. Breslin, "Optimized transformer design: Inclusive of high-frequency effects," *IEEE Transactions on Power Electronics*, vol. 13, no. 4, pp. 651-659, July 1998.

[18] C.P. Dick, A. Konig, R. W. De Doncker, "Comparison of three-phase dc-dc converters vs. single-phase dc-dc converters," *IEEE Power Electronics and Drive Systems*, pp. 217-224, 2007.

[19] G. G. Oggier, G. O. Garcia, A. Oliva, "Switching control strategy to minimize dual active bridge converter losses," *IEEE Transactions on Power Electronics*, vol. 24, no. 7, pp. 1826-1838, July 2009.

CHAPTER 2

IMPACT OF SOLID-STATE TRANSFORMER TOPOLOGIES ON THE HIGH-FREQUENCY TRANSFORMER DESIGN

2.1 Introduction

The idea of an AC-AC high-frequency link, which is the base for the SST concept, was first introduced by W. McMurray in 1968 [1]. Several topologies to realize a SST have been proposed since then in the literature and great efforts have been made to improve their efficiency and performance [2]-[9]. The first research efforts were focused on locomotive traction systems; however, the growing interest on the integration of distributed generation and energy storage systems into electric distributions systems has led to more research on suitable topologies for the SST implementation.

Therefore, this chapter presents an overview of SST topologies enabling features that provide desired additional functionalities for future energy systems [12]-[13]. The selected SST topologies are evaluated in order to determine their impacts upon the high- or medium-frequency transformer design. The main parameters are the applied excitation voltages, resulting currents, and leakage inductance requirements for maximum power transfer.

2.2 Review of SST Topologies

SST topologies can be broadly classified in the four categories proposed in [10] and shown in Fig. 2.1; namely, (a) single-stage topology with no DC link, (b) two-stage topology with HV DC link, (c) two-stage topology with LV DC link, and (d) three-stage topology with HV and LV DC link [10], [11].
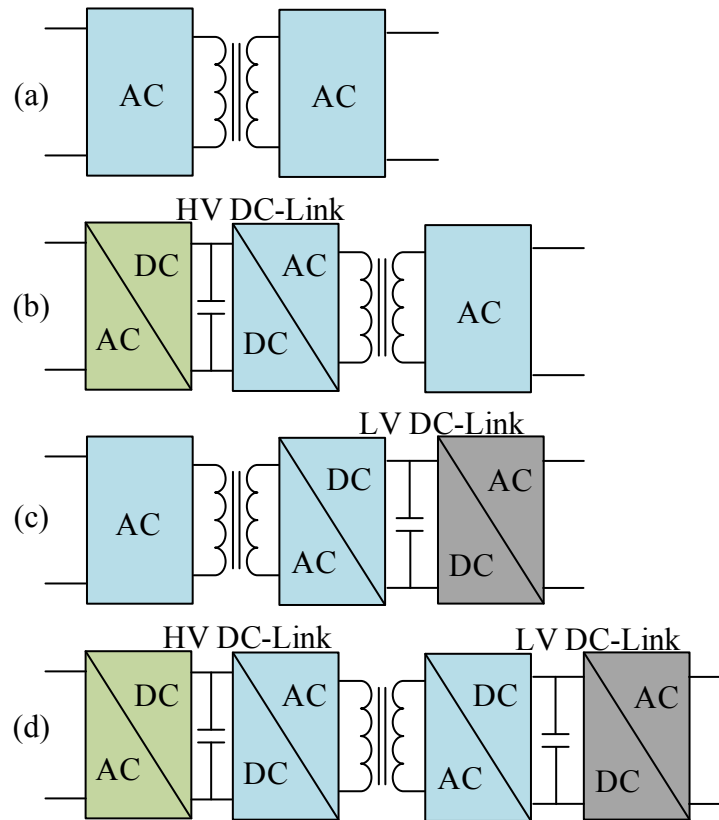
Fig. 2.1. Classification of SST topologies [10], [11]

Based on the functionalities that will be demanded by envisioned future energy systems, a suitable configuration for the SST implementation in distribution systems should meet the following minimum requirements:

- Available LV DC link for easy integration of renewable energies and energy storage elements [10]-[13].

- Modularity capability to improve reliability by adding levels of redundancy if desired, and to meet standard distribution voltage levels (input-series connection) and higher current ratings for high-power applications (output-parallel connection) due to the limitations of available switching devices [10]-[14].

- Unidirectional or bidirectional power-flow control functionality (i.e., on demand real and reactive powers) [10]-[13].

- Reduced number of components which may lead to lower cost, volume, and weight [11]-[13].

- Soft-switching operation to achieve higher efficiency [12], [13].

The topologies under (a) consist of a direct isolated AC-AC stage which might have the lowest cost and simplest approach among the other configurations. In addition, bi-directionality could be possible with four-quadrant switching devices. However, no DC links are available, thus reactive power compensation is not possible. In (b), an AC-DC conversion stage which provides a HV DC link is combined with a second stage DC-AC stage with galvanic isolation. Disturbance cancellation and reactive power compensation functionalities are possible with this configuration. Nonetheless, the lack of a LV DC link in (a) and (b) makes them unsuitable for applications in distribution systems where easy integration of renewable energies, and energy storage elements are desired [10]-[12].

Topologies under categories I and (d) overcome the limitation of an unavailable LV DC link. In I, an isolated AC-DC stage is followed by a DC-AC stage, thus a LV DC link is available. Category (d) includes topologies with a three-stage configuration combining an AC-DC stage followed by an isolated DC-DC stage and a DC-AC stage providing HV and LV DC link. Therefore, it can be concluded that, based on this classification, topologies under I and (d) are the best candidates for the SST implementation in distribution systems since they can provide all the required features expected from a SST [10]-[15]. In particular, (d) provides more controllability and flexibility since topologies for each of the three stages can be chosen from a variety of options

[10], [11]. The main disadvantage is the large number of components which may lead to higher cost, and lower efficiency and power density.

2.2.1 Description of Selected SST Topologies

Three SST topologies categorized as topology (d) (see Fig. 2.1) are selected in order to determine the impact imposes on the transformer. These topologies consist of three modules connected in series on the HV side and in parallel on the LV side. The number of modules is determined by the voltage blocking capability of 6.5 kV IGBTs as considered for the case study described in section 1.3. The selected topologies consist of AC-DC rectifiers switching at 1 kHz which convert 7.2 kV AC rms 60 Hz from the distribution grid to three 3.8 kV HV DC links. The interconnection of SSTs with a LV DC grid is considered; thus isolated bidirectional DC-DC converters step down the voltage to 400 V DC (LV DC link) with medium-frequency (MF) transformers which operate at 3 kHz.

The difference among the selected SST topologies for the case study is the realization of the DC-DC converter stage which leads to different voltages applied to the transformers, resulting currents, and leakage inductance requirements for maximum power transfer. Hence, each topology will require a different transformer design. The topologies consist of (I) full bridges on the HV and LV sides [11]-[13], (II) half bridges on the HV side and full bridges on the LV side [16], and (III) half bridges on the HV and LV sides [9], [14], as depicted in Figs. 2.2, 2.3, and 2.4, respectively.

In topology (I), when S_{1p} and S_{4p} are turned on, the voltage across the transformer primary winding, V_{T1}, is equal to the voltage in the HV DC link, V_1, thus $V_{T1} = V_1$. When S_{2p} and S_{3p} are on $V_{T1} = -V_1$. On the LV side, when S_{1s} and S_{4s} are on, the voltage across the transformer secondary winding, V_{T2}, is equal to the voltage in the LV DC link, V_2, thus $V_{T2} = V_2$ and $V_{T2} =$

14

$-V_2$ when S_{2s} and S_{3s} are ON. Therefore, the voltage applied to the primary and secondary of the transformer in a full-bridge converter is equal to the HV and LV DC link, respectively [17].
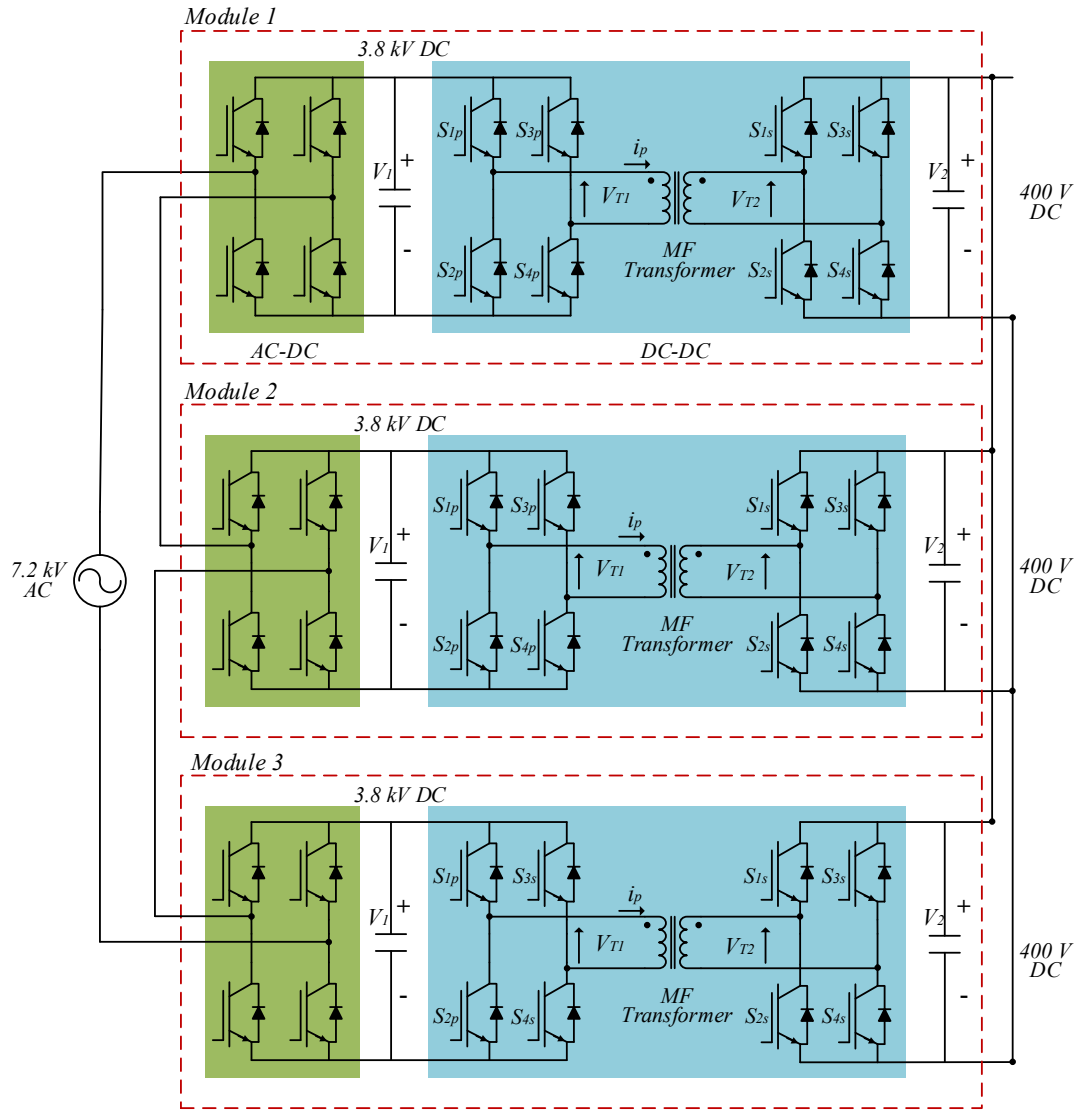
Fig. 2.2. SST topology with full bridges on HV and LV sides (I)
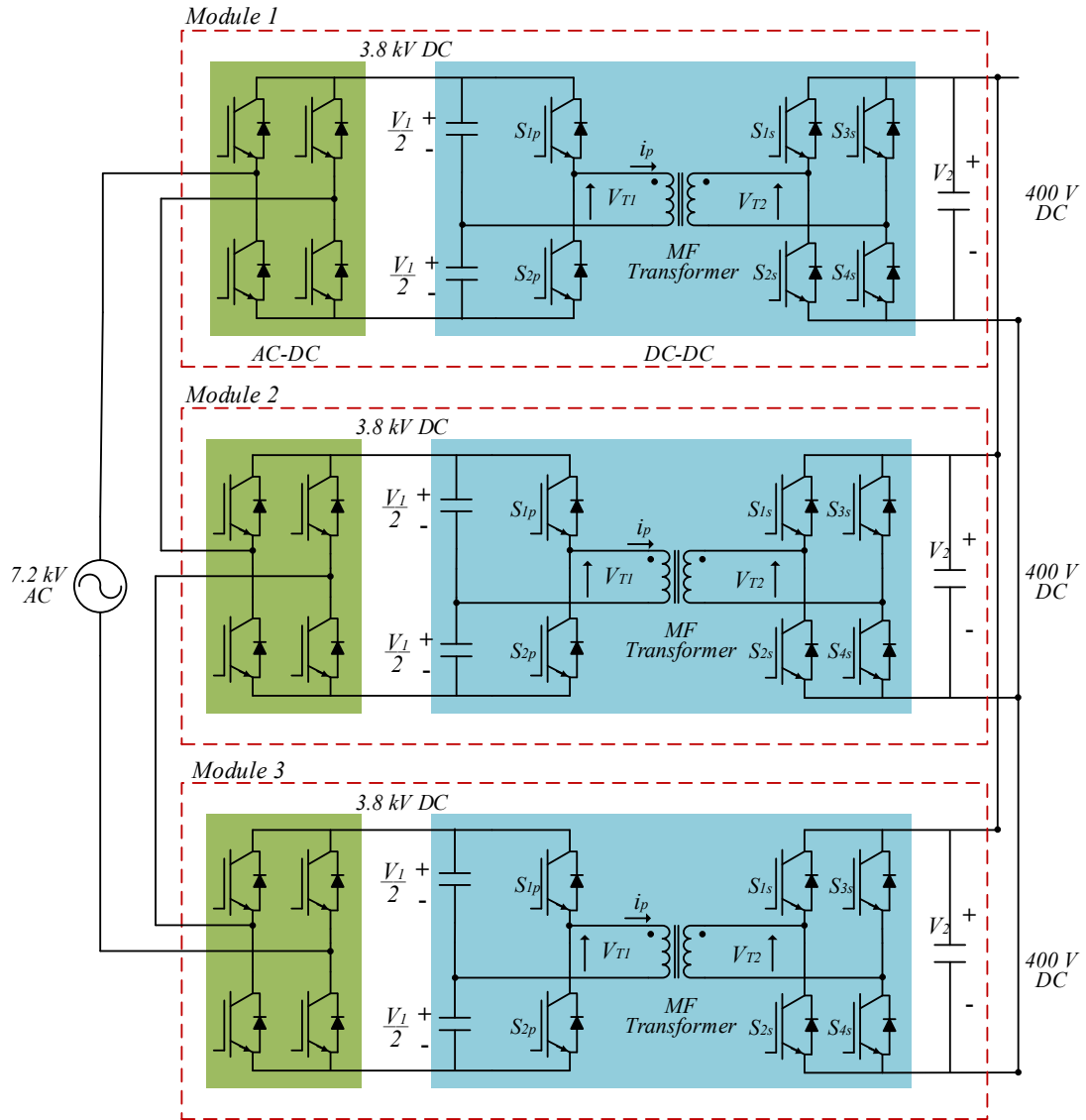
Fig. 2.3. SST topology with half bridges on HV side and full bridges on LV side (II)
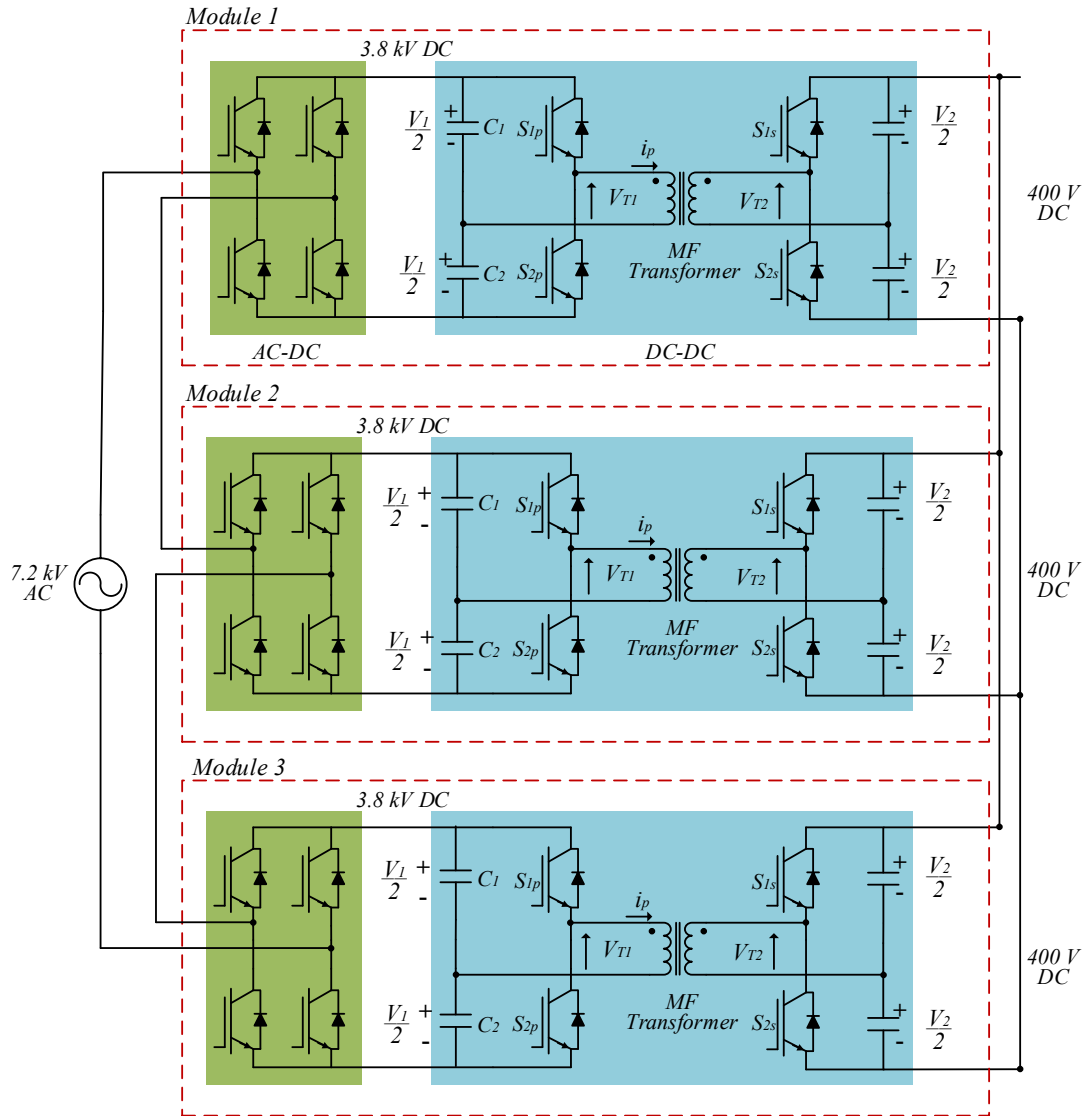
Fig. 2.4. SST topology with half bridges on HV and LV sides (III)

In topology (II), a half-bridge converter is used in the HV side; therefore, two transistors are replaced by two capacitors when compared with the full-bridge converter [17]. The voltage applied to the transformer is now half the total DC link voltage on the primary side, then $V_{T1} = V_1/2$. However, the current through the transformer primary winding and switching devices is twice the current in a full bridge for the same power rating [12]. In topology (III), half bridge converters are used on the HV and LV sides; therefore, the voltage applied to the transformer on

17

the primary side is $V_{T1} = V_1/2$ and to the secondary side is $V_{T2} = V_2/2$. Consequently, the currents through the primary and secondary windings are twice the currents in topology (I) [17].

The main specifications of the selected topologies based on the considered case study are given in Table 2.1. The full-bridge converter imposes less current stresses on the transformer; however, the voltage stresses are higher compared with a half-bridge converter for the same amount of power, thus it could impose a higher isolation requirement [18]. This requirement should be considered in the transformer design since the total volume will greatly depend on the required isolation level [19].

2.3 Operating Principle of the DAB

The DC-DC converter stage formed by a DAB can be simplified by referring the secondary bridge to the primary side and representing the transformer by its leakage inductance, L_k, as depicted in Fig. 2.5 [20]-[22]. It is assumed a much larger magnetizing inductance compared with the leakage inductance, thus the magnetizing branch can be considered an open circuit. The transformer leakage inductance is used as the main energy storage and transfer element [20]-[23].

Table 2.1. Main topology specifications for the case study

SST Topology	Transformer Voltage (V)		Transformer Peak Current (A)		Power Rating Per Module (kVA)	Switching Device Count	
	HV	LV	HV	LV		HV	LV
I	3800	400	125	1000	200	24	12
II	1900	400	250	1000	200	18	12
III	1900	200	250	2000	200	18	6
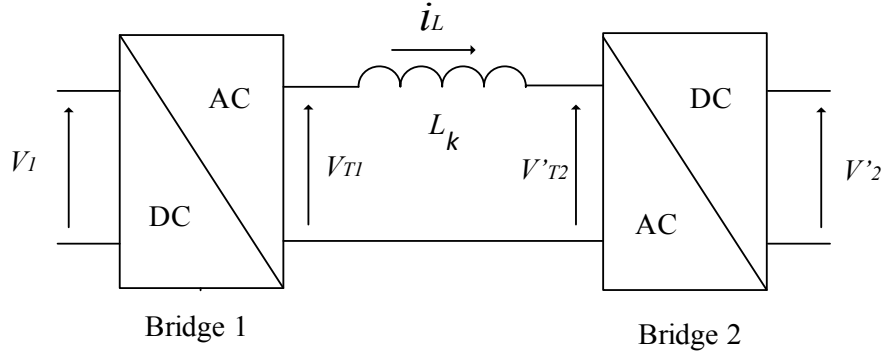
Fig. 2.5. Simplified representation of a DAB

The amount of power being transferred is determined by the phase shift between the primary and secondary voltages. Other modulation scheme that has been proposed in the literature is the combined phase-shift and pulse-width modulation (PSPWM) which have certain advantages over the traditional phase-shift modulation (PSM) [20]-[23]. The PSPWM method allows the extension of the zero-voltage switching (ZVS) operating range for wide input or/and output voltage variations, and reduces the transformer rms currents [20]-[23]. However, the traditional phase-shift modulation is a valid approach to analyze the impact that different SST topologies impose upon the transformer design; therefore, it is considered in this work.

The theoretical operating waveforms of the DAB with the PSM are given in Fig. 2.6, where $\theta = \omega t = 2\pi f_{sw} t$, f_{sw} is the switching frequency, δ is the inductor current i_L zero-crossing angle, ϕ corresponds to the phase-shift angle, and i_p is the primary current [20], [21].

The theoretical waveforms are applicable to any of the selected SST topologies and corresponds to the case where $V_{T1} > V_{T2}$ so power is transferred from bridge 1 to bridge 2 [15], [21]-[23].

19
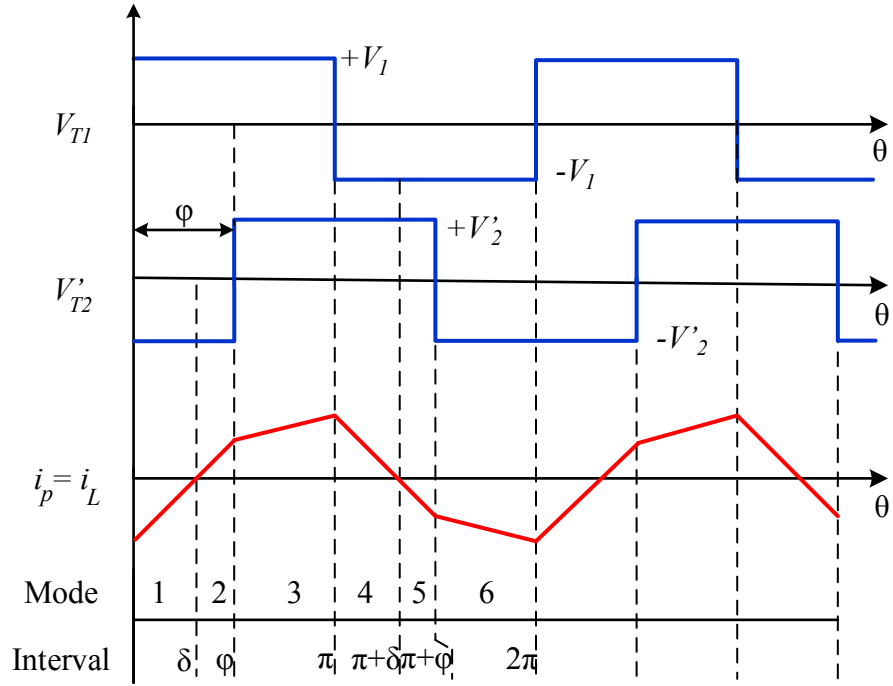
Fig. 2.6. Theoretical operating waveforms of a DAB

Each operating mode in Fig. 2.6 is described by a change in the state of a switching device which leads to six operating modes over one cycle. However, the current waveform is repeated every half cycle of the switching frequency due to symmetry; thus, it is only necessary to derive the equations for the inductor current for the intervals between mode 1 and mode 3 to determine the dynamics of i_L [15], [21]. The conducting switches for each interval, including the anti-parallel diodes D_{xx}, are given in Table 2.2 [15].

Table 2.2. Conducting switches in the DAB

$0 < \theta \leq \delta$		$\delta < \theta \leq \phi$		$\phi < \theta \leq \pi$	
Bridge 1	**Bridge 2**	**Bridge 1**	**Bridge 2**	**Bridge 1**	**Bridge 2**
D_{1p}	D_{2s}	S_{1p}	S_{2s}	S_{1p}	D_{1s}
D_{4p}	D_{3s}	S_{4p}	S_{3s}	S_{4p}	D_{4s}

For the simplified representation of the DC-DC converter stage shown in Fig. 2.5, the dynamics of i_L can be expressed as:

$$\frac{di_L(t)}{dt} = \frac{V_{T1}(t) - V_{T2}(t)}{L_k} \tag{2-1}$$

Solving (2-1) for i_L for each interval of the first half cycle and making use of the theoretical waveforms in Fig. 2.6, yields [15], [21]:

For $0 < \theta \leq \delta$

$$i_L(\theta) = \frac{V_1 + V_2'}{\omega L_k} \theta + i_L(0) \tag{2-2}$$

For $\delta < \theta \leq \phi$

$$i_L(\theta) = \frac{V_1 + V_2'}{\omega L_k} (\theta - \delta) + i_L(\delta) \tag{2-3}$$

For $\phi < \theta \leq \pi$

$$i_L(\theta) = \frac{V_1 - V_2'}{\omega L_k} (\theta - \phi) + i_L(\phi) \tag{2-4}$$

The initial condition $i_L(0)$ is calculated considering that the average value of i_L over one cycle must be equal to zero, hence $i_L(0) = -i_L(\pi)$ which results in:

$$i_L(0) = -\left[\frac{2V_2'\phi + \pi(V_1 - V_2')}{2\omega L_k}\right] \tag{2-5}$$

From Fig. 2.6, when $\theta = \delta$:

$$i_L(\delta) = 0 \tag{2-6}$$

Then, making (2-2) equal to zero at δ, yields

$$\delta = \left[\frac{2V_2'\phi + \pi(V_1 - V_2')}{2(V_1 + V_2')}\right] \tag{2-7}$$

Also, the instantaneous value, $i_L(\phi)$, is calculated from (2-3) for $\theta = \phi$:

$$i_L(\phi) = \frac{2V_1\phi - \pi(V_1 - V_2')}{2\omega L_k} \tag{2-8}$$

2.3.1 Maximum Power Transfer

Considering the equations describing the dynamics of i_L, and the applied primary and secondary voltages, the average transferred power can be obtained from [21]:

$$P_o = \frac{1}{T_s} \int_0^{T_s} V_{T1}(\theta)\, i_L(\theta) \tag{2-9}$$

where T_s is the switching period. Solving (2-9), the transferred power is calculated as:

$$P_o = \frac{V_1 V_2'}{\omega L_k \pi} \phi(\pi - \phi) \tag{2-10}$$

Hence, the magnitude and direction of power transfer are determined by the phase-shift angle, ϕ, between the primary and secondary voltages [20]-[23]. For $\phi > 0$, power is transferred from bridge 1 to bridge 2 [23]. For $\phi < 0$, power is transferred in the opposite direction. Moreover, ϕ for maximum power is determined by taking the derivative of (2-10) and equaling it to zero.

$$\frac{\partial P_0}{\partial \phi} = \frac{V_1 V_2'}{\omega L_k \pi} (\pi - 2\phi) = 0 \tag{2-11}$$

Then, the value of ϕ that corresponds to the maximum power transfer is:

$$\phi = \pm \frac{\pi}{2} \tag{2-12}$$

Therefore, the transferred power varies from zero to its maximum value for ϕ varying from 0 to $\pi/2$ [21], [23]. However, ZVS can only be achieved for the full-operating region when the voltage ratio equals 1 [22]. For a different voltage ratio, the ZVS range is reduced to a smaller operating region where maximum converter efficiency can be achieved [21]. Hence the advantage of the PSPWM control for wide input and/or output voltage ranges. However, the PSPWM can

22

only be implemented with topologies that can generate three-level transformer voltages on the primary and/or secondary sides [23], such as topology (I) and (II) shown in Figs. 2.2 and 2.3.

2.3.2 Leakage Inductance Requirement

Another important component to determine the amount of transferred power is the leakage inductance L_k, as illustrated in Fig. 2.5, which can be solved from (2-10). For the optimum condition in (2-12), the required inductance L_k for maximum power transfer is calculated as follows [15], [20]-[23]:

$$L_k = \frac{V_1 V_2'}{8 f P_o} \tag{2-13}$$

With (2-3) and the topology specifications in Table 2.1, the leakage inductance for each topology are calculated and the results given in Table 2.3. Each topology requires a different leakage inductance for its optimum operation. If this requirement is not fulfilled with the transformer design, an additional inductor might be needed to achieve the desired inductance, thus leading to a higher system volume and weight [24].

Table 2.3. Required leakage inductances for the case study

SST Topology	I	II	III
L_k (mH)	3.01	0.63	0.71

2.4 Conclusions

A review of SST topologies was presented in this chapter in order to stablish their suitability in envisioned future energy systems. It was concluded that those topologies consisting of two or three stages with a LV DC link are the most suitable for the SST implementation since they can provide the main features desired in future energy systems.

In particular, three SST topologies were considered in order to determine the requirements that they impose on the transformer design. For the same case study, different topologies can lead to different current and voltage stresses on the HF/MF transformer which has an impact on the isolation requirements and total transformer volume. Moreover, the leakage inductance of the transformer plays an important role in the power transfer per the operating principle of the DC-DC converter stage; thus, it was suggested that the transformer design include a leakage inductance specification to avoid the use of an external inductor in order to meet the series inductance required by each SST topology. Chapter 3 will focus on other considerations for designing HF/MF transformers.

2.5 References

[1]   W. McMurray, "Power converter circuits having a high-frequency link," U.S. Patent 3517300, June 23, 1970.

[2]   J. L. Brooks, "Solid state transformer concept development," in Naval Material Command. Port Hueneme, Civil Eng. Lab, Naval Construction Battalion Center, 1980.

[3]   "Proof of the principle of the solid-state transformer and the AC/AC switchmode regulator," San Jose State Univ., San Jose, CA, EPRI TR-105 067, 1995.

[4]   M. Kang, P. N. Enjeti, and I. J. Pitel, "Analysis and design of electronic transformers for electric power distribution system," in *Proceedings of the IEEE Industry Applications Conference*, IAS, vol. 2, pp. 1689-1694, Oct. 1997.

[5]   E. R. Ronan, S. D. Sudhoff, S. F. Glover, and D. L. Galloway, "A power electronic-based distribution transformer," *IEEE Transactions on Power Delivery*, vol. 17, no. 2, pp. 537–543, April 2002.

[6]   J. S. Lai, A. Maitra, A. Mansoor, and F. Goodman, "Multilevel intelligent universal transformer for medium voltage applications," in *Proceedings of the IEEE Industry Applications Conference*, IAS, vol. 3, pp. 1893–1899, Oct. 2005.

[7]   K. Harada, F. Anan, K. Yamasaki, et al. "Intelligent transformer", in *Proceedings of the IEEE 32nd Annual Power Electronics Specialists Conference*, PESC, vol. 2, pp. 1337-1341, 2006.

[8]   L. Y. Yang, T. F. Zhao, J. Wang, and A. Q. Huang, "Design and analysis of a 270 kW five-level dc/dc converter for solid state transformer using 10 kV SiC power devices," in *Proceedings of the Power Electronics Specialists Conference*, PESC, pp. 245–251, Jun. 2007.

[9]   D. Dujic, F. Kieferndorf, F. Canales, U. Drofenik, "Power electronic traction transformer technology," in *Proceedings of the 7th IEEE International Power Electronics and Motion Control Conference*, IPEMC 2012, China, pp. 636–642, Jun. 2-5, 2012.

[10] L. Heinemann and G. Mauthe, "The universal power electronics based distribution transformer, an unified approach," in *Proceedings of the IEEE 32nd Annual Power Electronics Specialists Conference*, PESC, vol. 2, pp. 504–509, 2001.

[11] S. Falcones, X. Mao, R. Ayyanar, "Topology Comparison for Solid State Transformer Implementation," *IEEE Power and Energy Society General Meeting*, pp. 1-8, Jul. 2010.

[12] T. Zhao, "Design and control of a cascaded h-bridge converter based solid state transformer (SST)," Ph.D. dissertation, Dept. Elect. Eng., North Carolina State Univ., Raleigh, North Carolina, USA, 2010.

[13] X. She, A. Q. Huang, R. Burgos, "Review of solid-state transformers technologies and their application in power distribution systems," *IEEE Journal of Emerging and Selected Topics in Power Electronics*, vol. 1, no. 3, pp. 186-198, Sept. 2013.

[14] S. Hwang, X. Liu, J. Kim, H. Li, "Distributed digital control of modular-based solid-state transformer using DSP+FPGA," *IEEE Transactions on Industrial Electronics*, vol. 60, no.2, Feb. 2013.

[15] K. D. Hoang, J. Wang, "Design optimization of high-frequency transformer for dual active bridge dc-dc converter," *Electrical Machines (ICEM), 2012 XXth International Conference*, pp. 2311-2317, Sept. 2012.

[16] Y. Huina, X. Wang, W. Gang, "Design of Electronic Transformer Used in a Proposed Circuit Topology for PET," *Power and Energy Engineering Conference*, 2012 Asia-Pacific, pp. 1-4, Mar 2012.

[17] V. Dmitri, J. Tanel, E. Mikhail, "Feasibility study of half- and full-bridge isolated dc/dc converters in high-voltage high-power applications," *13th International Power Electronics and Motion Control Conference*, 2008, pp. 1257-1261, Sept. 2013.

[18] H. Fan, H. Li, "High-frequency transformer isolated bidirectional dc-dc converter modules with high efficiency over wide load range for 20 kVA solid-state transformer," *IEEE Transactions on Power Electronics*, vol. 26, no. 2, pp. 3599-3608, Dec. 2011.

[19] G. Ortiz, J. Biela, J. W. Kolar, "Optimized design of medium frequency transformers with high isolation requirements," in *Proceedings of the 36th IEEE Industrial Electronics Society Conference*, IECON 2010, pp. 631-638, Nov. 2010.

[20] R. W. De Doncker, D. M. Divan, and M. H. Kheraluwala, "A three-phase soft-switched high-power-density dc/dc converter for high-power applications," *IEEE Transactions on Industry Applications*, vol. 27, no. 1, pp. 63–73, Jan./Feb. 1991.

[21] G. G. Oggier, R. Leidhold, G. O. Garcia, A. R. Oliva, J. C. Balda, F. Barlow, "Extending the zvs operating range of dual active bridge high-power dc-dc converters," in *Proceedings of the 37th IEEE Power Electronics Specialists Conference*, PESC 2006, pp. 1-7, Jun. 2006.

[22] G. G. Oggier, G. O. Garcia, A. R. Oliva, "Switching Control Strategy to Minimize Dual Active Bridge Converter Losses," *IEEE Transactions on Power Electronics*, vol. 24, no. 7, pp. 1826-1838, July 2009.

[23] F. Krismer, J. W. Kolar, "Efficiency-optimized high-current dual active bridge converter for automotive applications," *IEEE Transactions on Industrial Electronics*, vol. 59, no. 7, Jul. 2012.

[24] Y. Du, S. Baek, S. Bhattacharya, A. Q. Huang, "High-voltage high-frequency transformer design for a 7.2kV to 120V/240V 20kVA solid state transformer," in *Proceedings of the 36th Annual Conference on IEEE Industrial Electronics Society*, IECON 2010, pp. 493-498, Nov. 2010.

CHAPTER 3

DESIGN CONSIDERATIONS OF HIGH- OR MEDIUM-FREQUENCY

TRANSFORMERS

3.1 Introduction

The main components of a SST topology are the power converters and the high- or medium-frequency transformers. In Chapter 2, it was mentioned that there will be different impacts on the transformer depending on the selected topology to realize a SST. These must be considered within the transformer design (i.e., different current, voltage and leakage inductance requirements). Furthermore, other transformer design considerations must be investigated in order to achieve high efficiency and power density, which are desired features in a SST, and thus, to overcome the challenges of operating at high- or medium- frequencies. Hence, the main objective of this chapter is to present the design considerations for HF/MF transformers in order to establish the basics for the transformer design methodology which will be presented in Chapter 4.

To accomplish the above objective, a magnetic core characterization that defines a criteria for the core material selection, and an analysis of high-frequency effects on the transformer windings that leads to recommendations for the wire selection will be presented in this chapter. In addition, isolation requirements, as well as different transformer structures and techniques to achieve a required transformer leakage inductance will be presented.

3.2 Magnetic Core Characterization

Core material selection is critical in a transformer design since it impacts the cost, efficiency, and volume [1]-[3]. Therefore, it is important to understand the properties of the

magnetic materials. In particular, four properties can be used to characterize and properly select a core material suitable for certain application: core loss density (P_{fe}), saturation flux density (B_{sat}), relative permeability (μ_i), and Curie temperature (T_c) [4], [5]. Typical core magnetic materials considered for high-frequency high-power transformers are ferrite, silicon steel, amorphous, and nanocrystalline [3]-[6].

A comparison of selected magnetics materials in terms of the aforementioned properties is listed in Table 3.1. Ferrite material is commonly used for high-frequency applications since it has relatively low core-loss density and low cost; however, it has low saturation flux density (~0.4 T) [7] which would result in a heavy and bulky transformer if it is used for high-power applications. Alternatively, standard silicon steel material has high saturation flux density (~1.5 T), high permeability, and high Curie temperature which are suitable properties for high-power applications [6], [8]. The main drawback of this material is its high core loss density under high-frequency operation due to eddy current losses. For that reason, some manufacturers provide cores made of advanced silicon steel with very thin laminations in order to be used in high- or medium-frequency applications and minimize eddy current losses. For instance, a transformer rated 2.2 MVA, 1 kHz was fabricated using silicon steel laminations with a thickness of 0.18 mm as reported in [9].

Amorphous material has gained a lot of interest in high-frequency high-power applications mainly due to its high saturation flux density (~1.56 T), and much lower core-loss density compared with the standard silicon steel while their costs are comparable [10]. Therefore, amorphous material offers a good balance between cost, efficiency, and power density [3]-[6]. Finally, the nanocrystalline material shows the best performance in terms of efficiency and power density since it has high saturation flux density (~1.2 T) and the lowest core-loss density [11].

Table 3.1. Comparison of magnetic material properties

Parameter	Ferrite 3C94 [7]	Silicon Steel Arnon 7 [8]	Amorphous Metglas 2605SA1 [10]	Nanocrystalline Vitroperm 500F [11]
P_{fe} (W/kg) @ 20 kHz, 0.2 T	< 18	< 400	< 40	< 8
B_{sat} (T)	0.47	1.53	1.56	1.2
T_c (°C)	220	730	399	600
Permeability @ 20 kHz, μ_i	2 k	16 k	10 k-150 k	20 k

However, the nanocrystalline material has a considerable higher manufacturing cost which limits its use in high-power applications. Moreover, the standard shape of nanocrystalline cores is toroidal tape-wound which imposes a limitation on the transformer construction [5], [6]. Some manufacturers produce special nanocrystalline core shapes with further manufacturing processes; however, the effects of those extra processes on the material properties must be investigated; see for example [5].

In conclusion, cores made of thin silicon steel laminations, amorphous or nanocrystalline are the most suitable for the considered SST applications; however, the final selection depends on the designer criteria when considering design tradeoffs as represented in Fig. 3.1. For example, if the main design goals are high efficiency and power density, the transformer cost will be compromised. However, high efficiency could be achieved at a lower cost by decreasing power density.
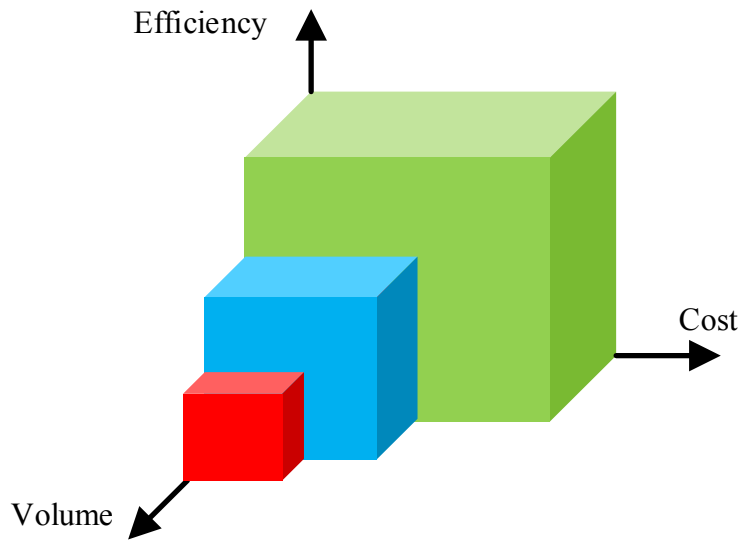
Fig. 3.1. Tradeoffs between cost, efficiency, and volume

3.3.1 Transformer Core Losses

A closer look to the core losses is addressed in this section in order to further understand the magnetic material characterization. The core losses in a magnetic material are mainly constituted by hysteresis loss, eddy current loss, and residual loss [5]. The hysteresis loss is related to the re-orientation of the magnetic domains. If a magnetic field intensity H is applied to the magnetic material, it will follow path (1) in Fig. 3.2 until it reaches the saturation flux density B_{sat}. If the field is reduced, the material will follow path (2). When the field is zero, the magnetic material retains a fraction of the magnetization which is the remanence flux density B_r. In order to bring the flux density to zero, a coercive field, labeled as H_c, must be applied. If the field is further increased in the negative direction, the material would again reach saturation, but in the opposite direction. Then the material will follow path (3) and close the hysteresis loop. Each time the magnetic field changes its direction, energy is expended in the re-orientation of the domains in the

magnetic material [1], [5], [12]. This energy is the hysteresis loss which is proportional to the area of the hysteresis loop shown in Fig. 3.2.

Another type of losses in the core is the eddy-current loss which is due to the induced voltage within the magnetic core in the same way that it is induced across the windings as explained by Faraday's law. This voltage produces currents that flow in a resistive environment.

In order to minimize eddy-current loss, the paths where the currents flow within the core have to be reduced [12]. For that reason magnetic cores are made with laminations which reduce the trajectory of the currents [1]. The major percent of the total core losses is due to hysteresis and eddy-current losses; the rest is attributed to the residual losses which are losses with a more complex mechanism and often related to the relaxation process in the magnetic material [12].
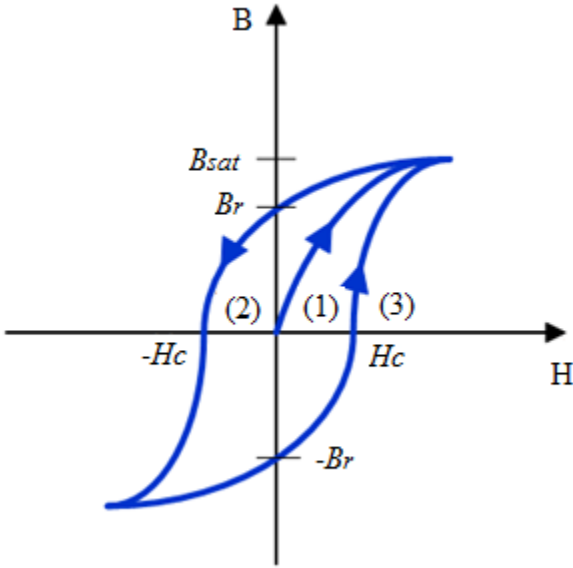
Fig. 3.2. Hysteresis loop

3.3.2 Core Loss Calculation Methods

Several approaches to determine the core losses have been proposed in the literature [13]-[15]. The separation of losses as explained in section 3.3 is one of the approaches used to determine the core losses [13]. Other approaches are based on hysteresis modeling such as the Preisach model and Jiles-Atherton model [14], [15]. Although those approaches can be very accurate, extensive calculations and measurements are required in order to get a core loss estimation [15]. Therefore, empirical equations based on measured data are more commonly used to estimate core losses [5], [14], [15]. Particularly, a widely used equation is the Original Steinmetz Equation (OSE):

$$P_v = Kf^\alpha B_m^\beta \qquad\qquad (3\text{-}1)$$

where P_v is the time-average power loss per unit volume; K, α and β are material parameters obtained from manufacturer's datasheet or determined by curve fitting the material loss curve under sinusoidal excitation; and B_m is the maximum flux density resulting from an excitation voltage with frequency f.

The limitation of the OSE is that it is only applicable to sinusoidal excitations [14]-[17]; therefore, it is not valid for most cases in power electronics where typically the magnetic material is excited with nonsinusoidal waveforms. For instance, the modulation strategy described in section 2.3 to operate the DAB converter leads to rectangular waveforms in both primary and secondary windings of the transformer.

Several modifications to the OSE have been proposed to overcome this limitation [15]. For instance, the Modified Steinmetz Equation (MSE) relates the rate of change of the flux density (*dB/dt*) to the core losses and replace the frequency *f* in the OSE for an equivalent frequency f_{eq} given by [16]:

$$f_{eq} = \frac{2}{\Delta B^2 \pi^2} \int_0^T \left(\frac{dB}{dt}\right)^2 dt \qquad (3\text{-}2)$$

where ΔB is the peak-to-peak flux density and T is the period of the excitation waveform. With (3-2) the

core loss under nonsinusoidal excitations can be estimated from [15], [16] as follows:

$$P_v|_{\text{MSE}} = \left(K f_{eq}^{\alpha-1} B_m^{\beta}\right) f_r \qquad (3\text{-}3)$$

where f_r is the fundamental frequency of the excitation waveform.

Although this modification have shown accuracy for some nonsinusoidal waveforms [16],

experimental validations prove that it cannot be generalized for all arbitrary waveforms [17]. In

fact, it does not match with the OSE when having sinusoidal waveforms [17]. Therefore, the

Generalized Steinmetz Equation (GSE) was proposed to overcome the limitations of the MSE.

The basics for the GSE is that the core-loss density depends not only on the rate of change

of the flux density, but also on its instantaneous value $B(t)$ which leads to the following expression

for loss calculation [17]:

$$P_v|_{\text{GSE}} = \frac{1}{T} \int_0^T k_1 \left|\frac{dB(t)}{dt}\right|^{\alpha} |B(t)|^{\beta-\alpha} dt \qquad (3\text{-}4)$$

$$k_1 = \frac{K}{(2\pi)^{\alpha-1} \int_0^{2\pi} |\cos\theta|^{\alpha} |\sin\theta|^{\beta-\alpha} d\theta} \qquad (3\text{-}5)$$

where the expression for k_1 is obtained by solving (3-4) for a sinusoidal excitation case and

equating the result with the OSE (3-1) [17].

Although the GSE is consistent with the OSE, it does not consider the material time history

for the estimation of the power loss density; therefore, it is highly inaccurate when having minor

hysteresis loops [18]. For that reason, an improved version of the GSE was proposed, the so called

Improved Generalized Steinmetz Equation (iGSE) [17], where the instantaneous values of the flux

density in the GSE are replaced by peak-to-peak values of the flux density ΔB in order to account for both major and minor hysteresis loops, yielding [14], [17]:

$$P_v|_{\text{iGSE}} = \frac{1}{T} \int_0^T k_i \left| \frac{dB(t)}{dt} \right|^\alpha (\Delta B)^{\beta - \alpha} dt \tag{3-6}$$

$$k_i = \frac{K}{(2\pi)^{\alpha - 1} \int_0^{2\pi} |\cos \theta|^\alpha 2^{\beta - \alpha} d\theta} \tag{3-7}$$

However, the main drawbacks of the iGSE are that first, it does not account for core loss under DC bias condition and second, it does not consider the relaxation process which occurs when having waveforms with zero-voltage conditions [14]. In fact, for all the aforementioned calculation methods proposed for arbitrary waveforms, it is assumed that the losses are zero during constant flux density, but experimental results demonstrate that even during this condition losses can occur hypothetically due to magnetic relaxation [14].

The inaccuracies of the iGSE are investigated in [12] and experimental verifications show that for very small duty cycles (D < 0.2) (i.e., wider zero-voltage condition) the calculated losses with the iGSE are under estimated [4], [14]. Therefore, the authors proposed an improved core-loss calculation method named the Improved-Improved Generalized Steinmetz Equation (i²GSE) that accounts for the losses during magnetic relaxation [14].

Despite the inaccuracies of the iGSE for very small duty cycles, this approach is still widely used in magnetic core loss characterization, since the core-loss density can be calculated for arbitrary waveforms, minor hysteresis loops are accounted for, and only Steinmetz coefficients obtained from manufacturer's datasheet are required [17], [18]. Moreover, it is anticipated that for the considered case study the duty cycles are around 50% where the iGSE can be as accurate as the i²GSE [14].

3.3.3 Selection of a Core-Loss Measurement Method

To this end, it can be noticed that core losses can depend on multiple factors. For example, temperature, excitation waveform, DC bias conditions, and relaxation effects. Therefore, the best way to properly estimate the core losses is to compare the calculations obtained from empirical equations with measurements. Hence, several core-loss measurement techniques have been proposed in an effort for improving the accuracy of the measurements [19]-[22].

A comparison of different core-loss measurement techniques is presented in [22] where it can be concluded that some of the most desired features of an effective measurement technique are the following:

- Winding loss can be separated from core-loss measurements

- Easy implementation and fast measurements

- Applicable to arbitrary waveforms

- Error due to phase discrepancy is minimum

Among the core-loss measurement techniques evaluated in [22], the wattmeter or two-winding method shown in Fig. 3.3 is one of the most popular ones. The steps to obtain the core loss with this method are [4], [21], [22]:

a) With the secondary winding in open circuit, measure the current i_p flowing through the excitation or primary winding. This current can be measured directly with a current probe or indirectly by sensing the voltage v_r across the reference resistor R_{ref}, and then applying Ohm's Law.

b) Measure the voltage across the secondary winding v_s.

c) Integrate the product of the excitation current waveform and the secondary voltage waveform, as given by (3-8):
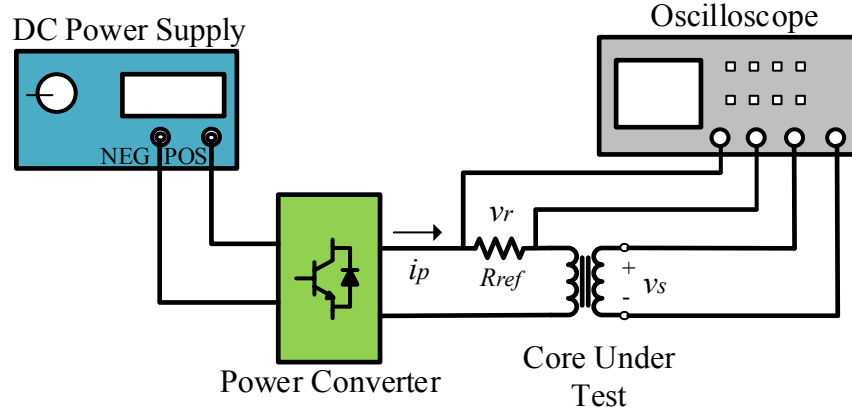
Fig. 3.3. Schematic of the two-winding method

$$P = \frac{1}{T} \int_0^T \frac{N_p}{N_s} v_s(t) . i_p(t) dt \qquad (3\text{-}8)$$

where N_p and N_s are the number of primary- and secondary-winding turns, respectively. For

convenience, N_p and N_s could be made equal ($N_p = N_s$).

The main advantages of this method are that the winding losses are excluded from the

measurements, it is applicable to arbitrary waveforms (e.g., two- or three- level square

waveforms), and only takes three steps to be implemented. However, this method is highly

sensitive to phase discrepancies which are more significant at high frequencies (> 1 MHz) [22].

Aware of this drawback, new measurement methods have been proposed, such as the capacitive

cancellation for sinusoidal waveforms and the inductive cancellation for non-sinusoidal

waveforms [22].

3.3.4   Core-Loss Measurements on Selected Magnetic Materials

A core-loss comparison of three soft-magnetic materials (ferrite, amorphous, and

nanocrystalline), whose properties are listed in Table 3.1, was presented in [4] as a result of this

thesis work. The comparison consists of an evaluation of losses at the frequencies of 10, 20, 50,

and 100 kHz, and duty cycles of 12.5, 25, 37.5, and 50%. It was considered a three-level excitation voltage waveform, as shown in Fig. 3.4.

The two-winding method described in section 3.3.3 was used for the core-loss measurements and a complete description of the test bench is given in [4]. The results were compared with the values calculated with the iGSE (3-6). The peak-to-peak flux density ΔB is obtained per Fig. 3.4 as follows:

$$\Delta B = 2B_{max} = \frac{V_{max}}{NA_e}\frac{DT}{2} \tag{3-9}$$

where A_e is the effective core cross-sectional area, N is the number of turns, T is the period, and D is the duty cycle of the voltage waveform. Equation (3-9) was used to calculate the required excitation voltage to maintain a constant flux density of 0.1 T over the different excitation conditions (i.e., different frequencies and duty cycles).
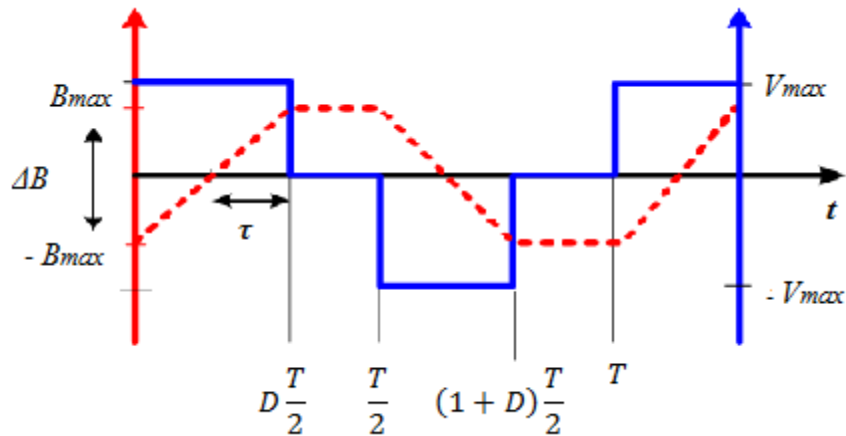
Fig. 3.4. Three-level excitation waveform

A piecewise linear model (PWL) was applied to the flux density waveform in Fig. 3.4 to calculate the rate of change of the flux density:

$$\frac{dB(t)}{dt} = \begin{cases} \dfrac{V_{dc}}{NA_e}, & 0 \leq t \leq D\dfrac{T}{2} \\ 0, & D\dfrac{T}{2} \leq t \leq \dfrac{T}{2} \\ -\dfrac{V_{dc}}{NA_e}, & \dfrac{T}{2} \leq t \leq (1+D)\dfrac{T}{2} \\ 0, & (1+D)\dfrac{T}{2} \leq t \leq T \end{cases} \tag{3-10}$$

Replacing (3-9) and (3-10) in (3-6) yields [1]:

$$P_v|_{\text{iGSE}} = k_i(\Delta B)^{\beta - \alpha} \frac{1}{T} \left[\int_0^{DT/2} \left| \frac{\Delta B}{DT/2} \right|^\alpha dt + \int_{DT/2}^{(1+D)T/2} \left| \frac{\Delta B}{DT/2} \right|^\alpha dt \right] \tag{3-11}$$

$$P_v|_{\text{iGSE}} = k_i(\Delta B)^{\beta - \alpha} \frac{1}{T} [|2\Delta B|^\alpha (DT)^{1-\alpha}] \tag{3-12}$$

An accurate approximation of the factor k_i was used to facilitate the calculations [1]:

$$k_i = \frac{K}{2^{\beta-1}\pi^{\alpha-1}\left(1.1044 + \dfrac{6.8244}{\alpha + 1.354}\right)} \tag{3-13}$$

The results from the comparison of the measured and calculated losses for the different selected materials and excitation conditions are given in the Appendix A.1. From the measurements, it can be observed that lower losses were obtained at 50% duty cycle and if the operating condition of $D = 50\%, f = 100\ kHz,$ and $B = 0.1\ T$ is selected from Fig. 3.5, it can be concluded that the ferrite 3C94 material responded with approximately 8 times higher losses than the nanocrystalline Vitroperm 500F, while the loss for the amorphous 2605SA1 is 1.5 times higher than the ferrite loss. These results match with the calculated values obtained with the iGSE.
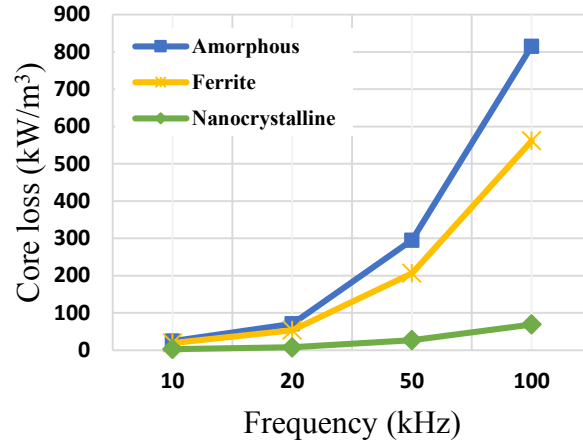
Fig. 3.5. Core losses of selected materials under different frequencies, D=50%, and B=0.1T

Another observation is that the calculated values with the iGSE showed more deviation from the measured values at very small duty cycles (<< 50%). This observation agrees with the conclusions presented in [14] and for that reason the i^{2}GSE was proposed to account for the relaxation effects. However, duty cycles around 50% are anticipated for the considered SST applications; therefore, accurate core loss estimation can be obtained with the iGSE.

3.3 High-Frequency Effects in Transformer Windings

The high-frequency effects in the core were addressed in previous sections and based on those effects, the magnetic core characterization and considerations for core material selection were given. However, it is also important to understand high-frequency effects in the windings; mainly skin and proximity effects which are illustrated in Fig. 3.6 and described in this section.

The DC resistance R_{DC} of the windings considering a conductor carrying a DC current or a low frequency AC current can be determined by:

$$R_{DC} = \frac{N.\rho.MLT}{A_w} \qquad (3\text{-}14)$$

where N is the number of turns of the winding, ρ is the specific resistance of the conductor, MLT is the mean-length of a turn, and A_w is the conductor cross-sectional area. Then, the winding loss can be easily calculated by multiplying the square of the current and R_{DC}.

Typically, only the DC resistance of a conductor is considered to calculate the winding losses; however, the resistance of a conductor at high frequencies increases because the current tends to flow only in the circumference and not in the whole conductor area; thus, the effective area of the conductor is reduced, and hence the AC resistance R_{AC} increases [23]. This phenomenon is known as the skin effect and is illustrated in Fig. 3.6(a).

The thickness of an equivalent conductor whose resistance equals the one of a solid conductor under skin effect is called skin depth δ and is calculated as follows [1], [2], [23]:

$$\delta = \frac{1}{\sqrt{\pi f \mu_o \sigma}} \tag{3-15}$$

where f is the operating frequency, σ is the specific conductivity of the conductor material, and μ_o is the permeability of the free space.
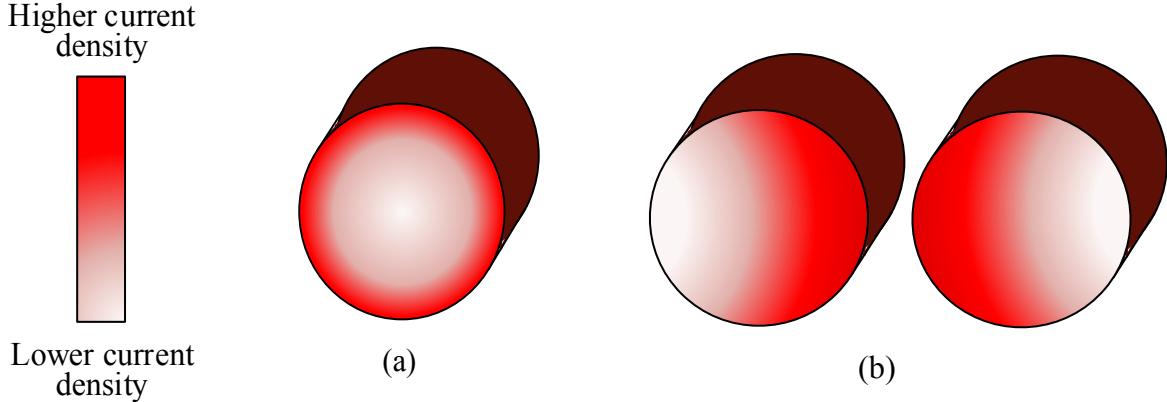
Fig. 3.6. Skin (a) and proximity effects (b) in windings

With (3-15), an equation that gives an approximate value of R_{AC} of a round conductor of radius r_o can be derived [1]:

$$R_{AC} = R_{DC}\left[1 + \frac{(r_o/\delta)^4}{48 + 0.8(r_o/\delta)^4}\right] \tag{3-16}$$

The skin effect is related to individual conductors; however, another high-frequency effect occurs in the presence of multiple conductors intertwined. This phenomenon known as the proximity effect is illustrated in Fig. 3.6(b). The AC resistance increases because of the interaction between opposing magnetic fields of conductors that are close to each other (i.e., current flows in opposite directions). This interaction causes the current in each conductor to be concentrated in a smaller area.

In order to reduce the skin and proximity effects in the windings, a stranded wire with insulated strands named Litz wire is commonly used [1], [2]. Also, foil plates could be used, but this option might not be suitable for high-power applications since the width of the plates could be excessively large [23]. Hence, Litz wire is recommended for the considered SST application.

3.4 Isolation Requirements

Since the SST is being proposed as a replacement of the traditional transformer, it must be in compliance with the international standards related to the requirements for distribution and power transformers, for example, the ANSI/IEEE C57.12.01. One of those requirements is the isolation level based on the transformer excitation voltage. This is a design consideration that must be included in the design since it will have a significant impact on the transformer power density.

The isolation level can be included within the transformer design through the calculation of a minimum isolation distance given by [3], [24]:

$$d_{i,min} = \frac{V_{iso}}{k_{iso}E_{ins}}$$
(3-17)

where V_{iso} is the isolation voltage level, E_{ins} is the dielectric strength of the insulation material, and k_{iso} is a safety margin given by some manufacturers or chosen based on the designer criteria. Properties of typical dry-type dielectric materials used in transformers are listed in Table 3.2.

If a basic insulation level of 95 kV is considered for the case study described in section 1.3 in compliance with the ANSI/IEEE C57.12.01 and each module is rated at the same isolation level, a dielectric material such as EPOXI could be selected from Table 3.2 with E_{ins} = 15 kV/mm and k_{iso} = 40% [3]; thus, the minimum isolation distance will be 16 mm. As will be discussed in the next section, the isolation distance between windings can be adjusted in order to meet the transformer leakage inductance requirement [3], [24].

Table 3.2. Properties of typical dry-type insulation mediums [24], [25]

Dielectric Material	Thermal Conductivity (W/m.K)	Dielectric Strength, E_{ins} (kV/mm)	Dissipation Factor tan(δ)
Air	0.03 (@70°C)	3	0
EPOXI	0.25	15	0.02 (@100 kHz)
Mica	0.71	11-43	-
NOMEX	0.175 (@150°C)	27	0.005 (@60 Hz)

3.5 Integration of Leakage Inductance

The importance of the series inductance as the main energy transfer element in the DAB converter and the desired for integrating this inductance as the leakage inductance of the transformer in order to maximize power density was studied in Chapter 2. Therefore, this section describes ways in which the desired leakage inductance value can be achieved within the transformer design.

The integration of the leakage inductance will greatly depend on the transformer structure [26]. Fig. 3.7 shows two of the most common transformer structures that could be used in high-power high-frequency applications: core-type and shell-type [2], [6], [26].

In a core-type structure, shown in Fig. 3.7(a), each winding is wound one on a leg of the core and due to the inherit separation of the windings, high leakage inductance and better isolation between windings may be achieved [26]. However, it is not easy to estimate the leakage inductance with analytical methods since most of the leakage flux does not remain inside the core window

| (a) | (b) |
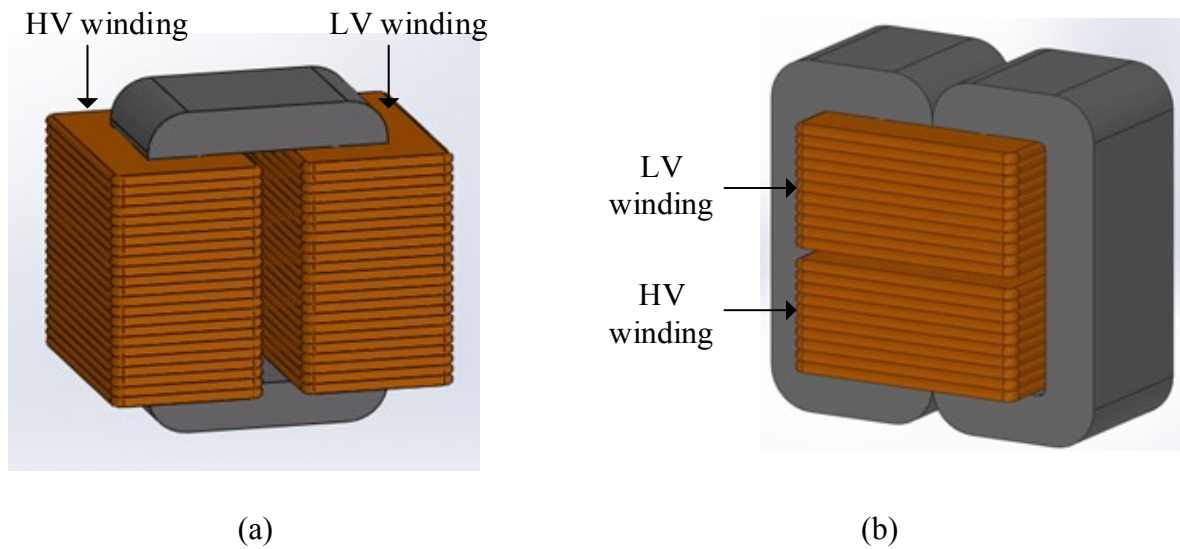
Fig. 3.7. Typical transformer structures: (a) core-type and (b) shell-type

area [26]; thus, 2D or 3D finite element simulations is preferred to estimate the leakage inductance in this type of structure [5], [26].

In a shell-type structure, shown in Fig. 3.7(b), both primary and secondary windings are wound in the center leg; therefore, lower leakage inductance might be achieved since the leakage flux remains within the window area. This makes easier and more precise the calculation of leakage inductance. Another important advantage of the shell-type structure is that most of the core surface area is exposed to the air which allows for better heat dissipation.

For the transformer in Fig. 3.8, the leakage inductance can be calculated considering the transformer geometric parameters as follows [2]:

$$L_k = \mu_o N^2 MLT . \frac{(a + b + 3c)}{3w} \tag{3-18}$$

where N is the number of turns corresponding to the winding which the leakage inductance is being calculated (primary or secondary), MLT is the mean length of a turn, μ_o is the air permeability, w is the core window width, a and b are the width of the primary and secondary windings, respectively, and c is the isolation distance between the windings.
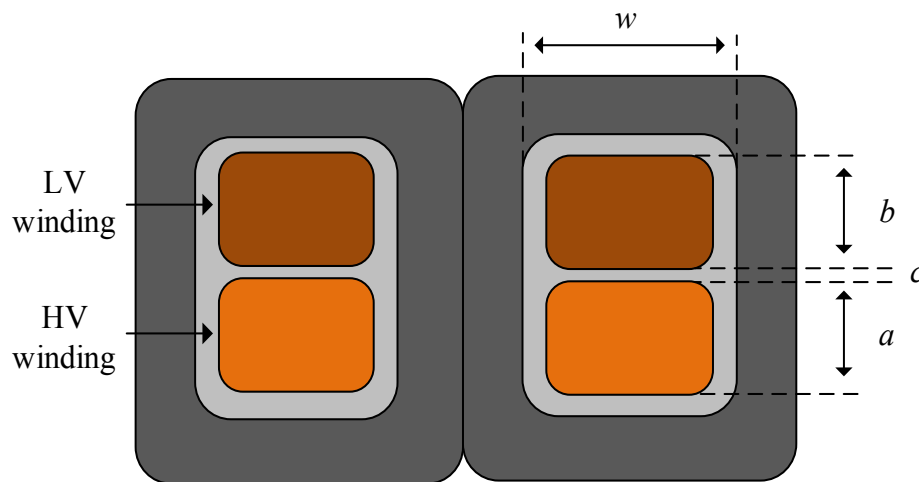
Fig. 3.8. Geometrical parameters for leakage inductance calculation

Based on (3-18) there are certain ways in which the leakage inductance could be adjusted according to the desired value as discussed below [26], [27]:

- Since the leakage inductance is proportional to the square of the number of turns, changing the number of turns (both primary and secondary windings to keep the same voltage ratio), is an effective way of increasing or reducing the leakage inductance.

- The isolation distance between windings has also a great impact on the leakage inductance; therefore, by varying the insulation thickness or clearance distance between windings, the leakage inductance can be adjusted. However, there is a lower limit imposed by the minimum isolation distance $d_{i,min}$ defined in (3-17).

- Further variations to the transformer structures given in Fig. 3.7 can vary the leakage inductance by using different winding arrangements. For example, the use of interleaved windings can be considered if the application requires low leakage inductance.

- A layer of a magnetic material with high permeability can be inserted between windings when a very high leakage inductance is desired and it cannot be achieved with the previous techniques. This method may be preferred instead of having an additional inductor [26].

3.6 Conclusions

Main design considerations for HF/MF transformer design were presented in this chapter. In particular, four main design aspects were discussed: core material selection, HF effects in windings, isolation level, and leakage inductance integration.

A review of the main core-loss calculation methods and a comparison of losses under different operating conditions with calculated values using the iGSE and measured values using the two-winding method were presented. It was concluded that amorphous and nanocrystalline materials are the most suitable for the considered SST application because of their high saturation flux density and low core loss density at the considered operating frequency (i.e., 3 kHz). Another potential candidate is the silicon steel material if the core is made of thin laminations in order to minimize eddy-current losses.

The HF effects in the windings lead to the use of special types of wires, such as Litz wire or foil plates in order to reduce skin and proximity effects, and hence reduce winding losses. These effects were studied and basic equations for selecting the appropriate wire size and estimating winding losses were given.

Moreover, the HV operation imposes a challenge in the transformer design for the power density optimization aspect since the SST has to meet the isolation requirements specified by international standards that are applicable to traditional 50/60 Hz transformers. For the case study, an isolation level of 95 kV was considered which resulted in a minimum isolation distance between windings of 16 mm.

Finally, the leakage inductance requirement as addressed in Chapter 2 was accounted for by presenting different techniques for the integration of the required inductance within the transformer design. One of these techniques is to adjust the isolation distance between windings in order to achieve the desired inductance.

The design considerations given in this chapter are taken into account in the proposed HF/MF transformer design methodology that will be described in Chapter 4.

3.7 References

[1] W. G. Hurley, W.H. Wölfle, Transformers and Inductors for Power Electronics: Theory, Design and Applications, 1st ed., Wiley, 2013.

[2] C. William, T. McLyman, Transformer and Inductor Design Handbook, 4th ed., Taylor & Francis Group, 2011.

[3] G. Ortiz, J. Biela, J. W. Kolar, "Optimized design of medium frequency transformers with high isolation requirements," in *Proceeding of the 36th IEEE Industrial Electronics Society Conference*, IECON 2010, pp. 631-638, Nov. 2010.

[4] R. Garcia, A. Escobar-Mejia, K. George, J.C. Balda, "Loss comparison of selected core magnetic materials operating at medium and high frequencies and different excitation voltages," in *Proceedings of the Power Electronics for Distributed Generation Systems*, PEDG 2014, pp. 1-6, June 2014.

[5] W. Shen, "Design of high-density transformers for high-frequency high-power converters," Ph.D. dissertation, Dept. Elect. Eng., Virginia Polytechnic Institute and State University, Blacksburg, Virginia, USA, 2006.

[6] X. She, A. Q. Huang, R. Burgos, "Review of solid-state transformers technologies and their application in power distribution systems," *IEEE Journal of Emerging and Selected Topics in Power Electronics*, vol. 1, no. 3, pp. 186-198, Sept. 2013.

[7] Ferroxcube, "Soft ferrites and accessories data handbook 2013," [Online]. Available: http://www.ferroxcube.com/FerroxcubeCorporateReception/datasheet/FXC_HB2013.pdf

[8] EMETOR, "Materials Library," [Online]. Available: https://www.emetor.com/edit/materials/arnon-7/ [Accessed April 2015].

[9] N. Soultau, H. Stagge, R. W. De Doncker, O. Apeldoorn, "Development and demonstration of a medium-voltage high-power DC-DC converter for DC distribution systems," in *Proceedings of the 5th IEEE International Symposium on Power Electronics for Distributed Generation Systems*, PEDG 2014, pp. 1-8, June 2014.

[10] Metglas®, "Powerlite® inductor cores technical bulletin," [Online]. Available: http://www.elnamagnetics.com/wp-content/uploads/catalogs/Metglas/powerlite.pdf [Accessed April 2015]

[11] [Online]. Available: http://www.vacuumschmelze.com/en/products.html [Accessed April 2015]

[12] J. B. Goodenough, "Summary of losses in magnetic materials," *IEEE Transactions on Magnetics*, Vol. 38, No. 5, pp. 3398-3408, Sept. 2002.

[13] F. Dong Tan, J. L. Vollin, S. M. Cuk, "A practical approach for magnetic core-loss characterization," *IEEE Transactions on Power Electronics*, Vol. 10, No. 2, pp. 124-130, March 1995.

[14] J. Mühlethaler, J. Biela, J.W. Kolar, A. Ecklebe, "Improved core-loss calculation for magnetic components employed in power electronic systems," *IEEE Transactions on Power Electronics*, vol. 27, no. 2, pp. 964–973, February, 2012.

[15] I. Villar, U. Viscarret, I. Etxeberria-Otadui, A. Rufer, "Global loss evaluation methods for nonsinusoidally fed medium-frequency power transformers," *IEEE Transactions on Industrial Electronics*, Vol.56, No. 10, pp. 4132-4140, Oct. 2009.

[16] J. Reinert, A. Brockmeyer, R.W. De Doncker, "Calculation of losses in ferro- and 48erromagnetic materials based on the modified Steinmetz equation", *IEEE Transactions on Industry Applications*, vo. 37, no. 4, July/August, 2001.

[17] J. Li, T. Abdallah, C.R. Sullivan, "Improved calculation of core loss with nonsinusoidal waveforms," in *Proceedings of the IEEE Industry Applications Society Annual Meeting*, pp. 2203–2210, October, 2001.

[18] K. Venkatachalam, C.R. Sullivan, T. Abdallah, H. Tacca, "Accurate prediction of ferrite core loss with nonsinusoidal waveforms using only Steinmetz parameters," in *Proceedings of the 8th IEEE Workshop on Computers in Power Electronics*, COMPEL 2002, pp.1–6, June 2002.

[19] M. Mu, Q. Li, "New core loss measurement method for high-frequency magnetic materials," *IEEE Trans. on Power Electronics*, vol. 29, no. 8, August 2014.

[20] J. Mühlethaler, J. Biela, J.W. Kolar, A. Ecklebe, "Core losses under the DC bias condition based on Steinmetz parameters," *IEEE Transactions on Power Electronics*, vol. 27, no. 2, pp. 953–963, February, 2012.

[21] Y. Han, Y. Liu, "A practical transformer core loss measurement scheme for high-frequency power converter," *IEEE Transactions on Industrial Electronics*, vol. 55, no. 2, February 2008.

[22] M. Mu, "High frequency magnetic core loss study," PhD. Dissertation, Dept. Elect. Eng., Virginia Polytechnic Institute and State University, Blacksburg, Virginia, USA, 2013.

[23] C. Meyer, "Key components for future offshore dc grids," PhD. Dissertation, RWTH Aachen University, Aachen, Germany, 2007.

[24] M. A. Bahmani, T. Thiringer, M. Kharezy, "Design methodology and optimization of a medium frequency transformer for high power dc-dc applications," in *Proceedings of the 30th Applied Power Electronics Conference and Exposition* (APEC), pp. 2532-2539, March 2015.

[25] [Online]. Available: http://www.dupont.com/content/dam/assets/products-and-services/electronic-electrical-materials/assets/DPP_Nomex410_K20612-1.pdf [Accessed April 2015]

[26] B. Cougo, J. W. Kolar, "Integration of Leakage Inductance in Tape Wound Core Transformers for Dual Active Bridge Converters," in *Proceedings of the 7th International Conference Integrated Power Electronics Systems* (CIPS), 2012, pp. 1-6, March 2012.

[27] P. A. Janse Van Rensburg, H. C. Ferreira, "The role of magnetizing and leakage inductance in transformer coupling circuitry," [Online]. Available: http://www.isplc.org/docsearch/Proceedings/2004/pdf/ISPLC04.pdf [Accessed April 2015]

APPENDIX A.1

CORE LOSS MEASUREMENTS OF SELECTED MAGNETIC MATERIALS UNDER

DIFFERENT EXCITATION CONDITIONS

As part of this thesis work, a core loss comparison of selected soft-magnetic materials operating at different frequencies, duty cycles and excitation voltages was performed and the results were published in [1]. The evaluated materials and their Steinmetz coefficients for the calculation of losses with the iGSE are listed in Table A.1. The calculated values were compared with measured losses using the two-winding method.

The comparison consists of an evaluation of core losses at the frequencies of 10, 20, 50, and 100 kHz, and duty cycles of 12.5, 25, 37.5, and 50% while keeping a constant flux density of 0.1 T. The results are shown in Figs. A.1 (Amorphous), A.2 (Ferrite), and A.3 (Nanocrystalline) where figures (a) are for 10 kHz, figures (b) for 20 kHz, figures (c) for 50 kHz, and figures (d) for 100 kHz.

Table A.1. Steinmetz coefficients for evaluated soft-magnetic materials

Parameter	Ferrite 3C94	Amorphous Metglas 2605SA1 (AMCC-80)	Nanocrystalline Vitroperm 500F (W630)
K (W/m^3)	17.1	1.3617	2.3
α	1.46	1.51	1.32
β	2.75	1.74	2.12

(a)

(b)

I
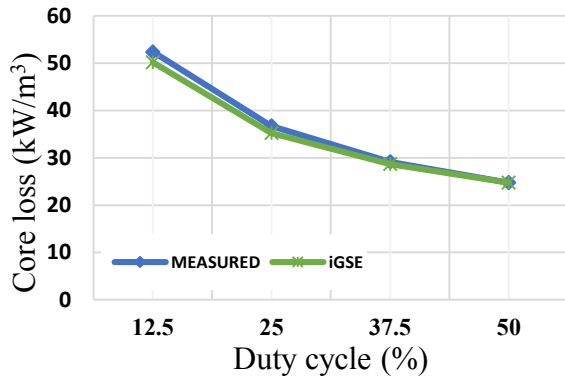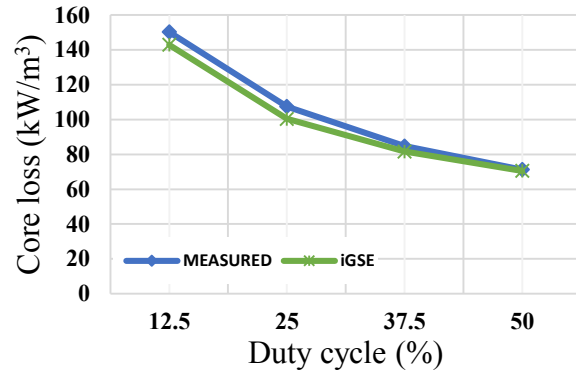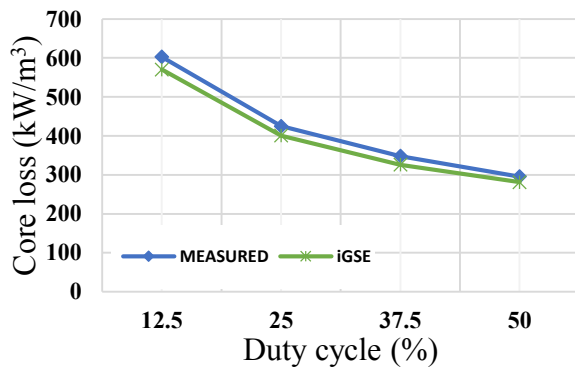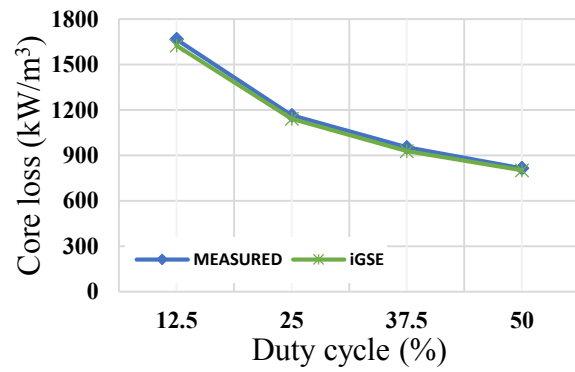
(d)

Fig. A.1. Amorphous (2605SA1) core losses for $f = 10\ kHz$ (a), $f = 20\ kHz$ (b), $f = 50\ kHz$ (c) and $f = 100\ kHz$ (d) at different duty cycles [1]
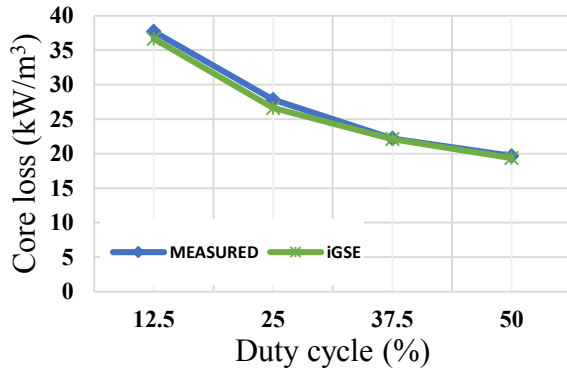
(a)
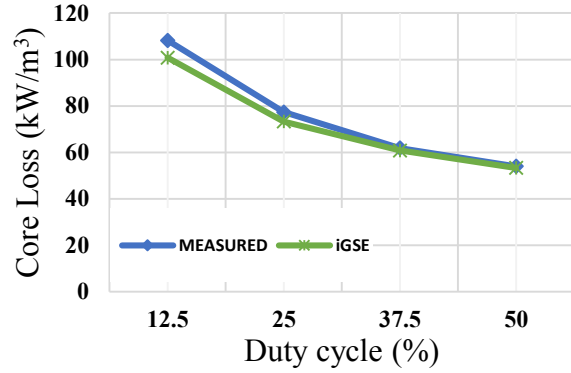
(b)
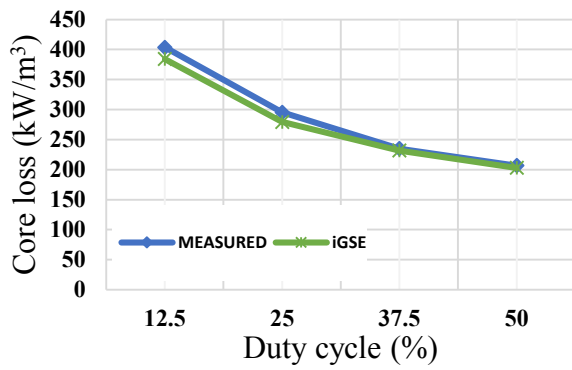
I
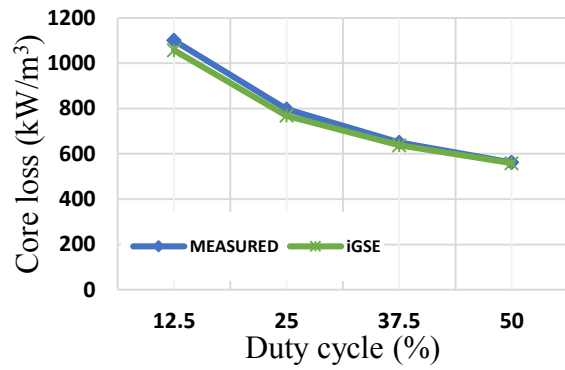
(d)

Fig. A.2. Ferrite core losses for $f = 10\ kHz$ (a), $f = 20\ kHz$ (b), $f = 50\ kHz$ (c) and $f = 100\ kHz$ (d) at different duty cycles [1]
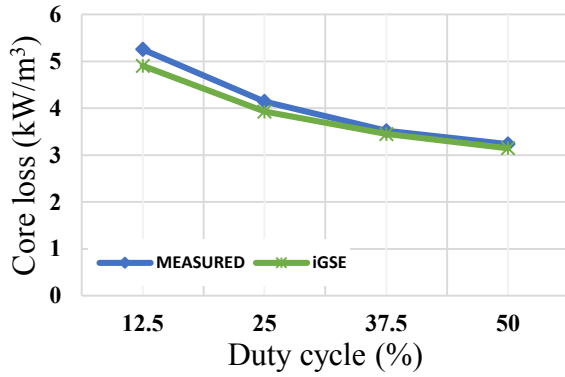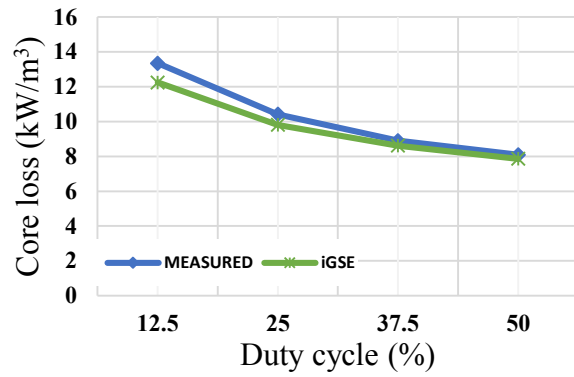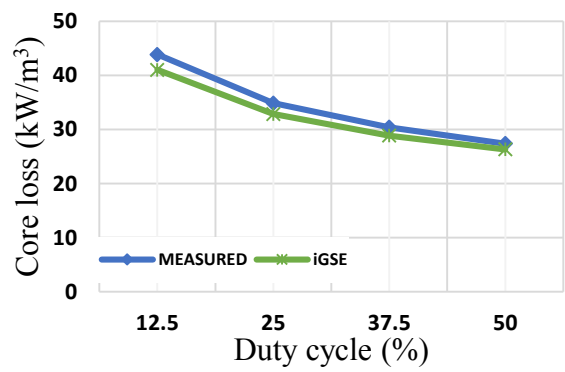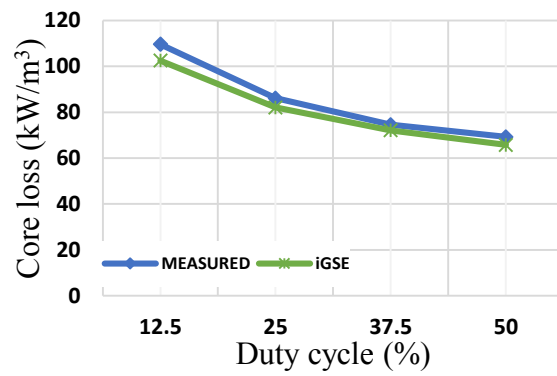
Fig. A.3. Nanocrystalline core losses for $f = 10\ kHz$ (a), $f = 20\ kHz$ (b), $f = 50\ kHz$ (c) and $f = 100\ kHz$ (d) at different duty cycles [1]

Reference

[1] R. Garcia, A. Escobar-Mejia, K. George, J.C. Balda, "Loss comparison of selected core magnetic materials operating at medium and high frequencies and different excitation voltages," in *Proceedings of the Power Electronics for Distributed Generation Systems*, PEDG 2014, pp. 1-6, June 2014.

CHAPTER 4

PROPOSED HIGH-FREQUENCY TRANSFORMER DESIGN METHODOLOGY

4.1 Introduction

As addressed in Chapter 1, the implementation of SSTs in high-voltage high-power applications introduces new challenges in the transformer design due to high-frequency, high-current, and high-voltage operations. The main considerations for designing HF/MF transformers were investigated in Chapters 2 and 3. Those considerations established the basics for the proposed single-phase HF/MF transformer design methodology that will be presented in this chapter.

The design methodology is applicable to transformer nonsinusoidal excitations that are typically encountered in power electronics, and considers the flux density optimization criteria presented in [1] to maximize the transformer's efficiency. The number of turns of the windings and the isolation distance between windings are used as free parameters to adjust the transformer leakage inductance required for maximum power transfer. An interactive tool using MATLAB® based on the proposed methodology is given in the Appendix B.1. The next section describes the optimization of the flux density adopted in this work.

4.2 Flux Density Optimization

High efficiency is one of the main desired characteristics of the HF/MF transformers for SSTs since the total system loss, unlike the traditional fundamental frequency transformer, will include the transformer losses, as well as the power converter losses (i.e., conduction and switching losses). Therefore, the transformer design procedure must be accompanied of a flux density

optimization criteria as the one described in [1] which has been adopted in this work to maximize transformer's efficiency.

The optimization criteria is based on two basic principles: (1) the winding loss P_{cu} is inversely proportional to the square of the frequency f and flux density B; i.e.,

$$P_{cu} \propto \frac{1}{f^2 B^2},\tag{4-1}$$

and (2) the core loss P_{fe} is proportional to f and B per the Steinmetz equation:

$$P_{fe} \propto f^\alpha B^\beta.\tag{4-2}$$

These principles are represented in Fig. 4.1. The total loss P_T is minimum at point A where it is assumed that the core and winding losses are approximately equal; hence, the starting point of the optimization criteria [1], [2].
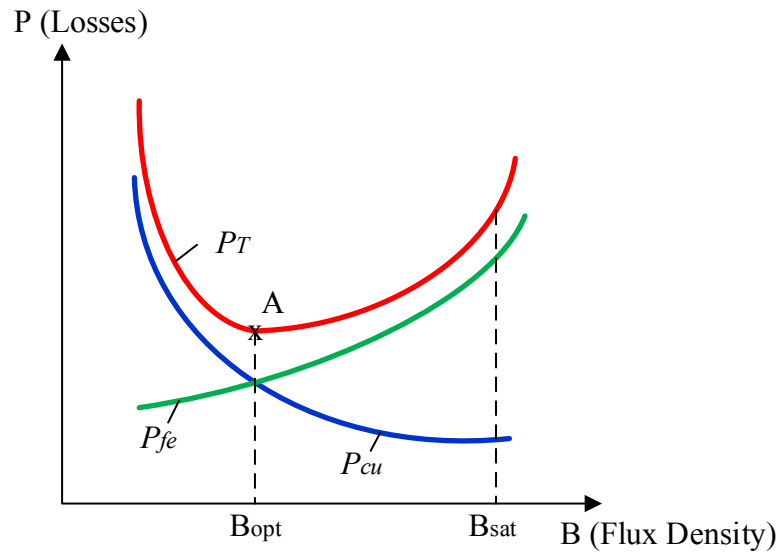
Fig. 4.1. Optimum flux density representation

Based on the aforementioned principles, the following equation to calculate the optimum flux density B_{opt} at point A (see Fig. 4.1) was derived in [1]:

$$B_{opt} = \frac{[h_c k_a \Delta T]^{2/3}}{2^{2/3}[\rho_w k_w k_u]^{1/12}[k_c K f^\alpha]^{7/12}}\left[\frac{K_v f k_f k_u}{\sum VA}\right]^{1/6} \tag{4-3}$$

where ρ_w is the wire resistivity; k_a, k_c, k_w, are dimensionless coefficients obtained from dimensional studies of different types of cores [1]; h_c is the coefficient of heat transfer; k_u the window utilization factor; $\sum VA$ the total transformer power rating; ΔT the temperature rise; K_v the waveform factor which depends on the shape of the voltage waveform applied to the windings; and k_f is the stacking factor which relates the effective cross-sectional area with the physical area of the core. Typical values of the coefficients and factors necessary to calculate B_{opt} will be given in the next section that presents the transformer design methodology proposed in this work.

4.3 High-Frequency Transformer Design Methodology

Besides the flux density optimization criteria, the proposed design methodology also includes the design considerations discussed in Chapter 3 in terms of the HF effects in the core and windings, as well as isolation and leakage inductance requirements. The proposed design flowchart is presented in Fig. 4.2 and was implemented in MATLAB® (Appendix B.1). Each design step is described next.

Step 1. System and Topology Specifications

This step introduces the following system specifications into the program: output power P_{out}, expected efficiency η, primary V_p and secondary V_s voltages, operating frequency f, temperature rise ΔT, and isolation level V_{iso}. Next, the topology specifications consisting of the

duty cycle D and the required leakage inductance L_k are introduced.
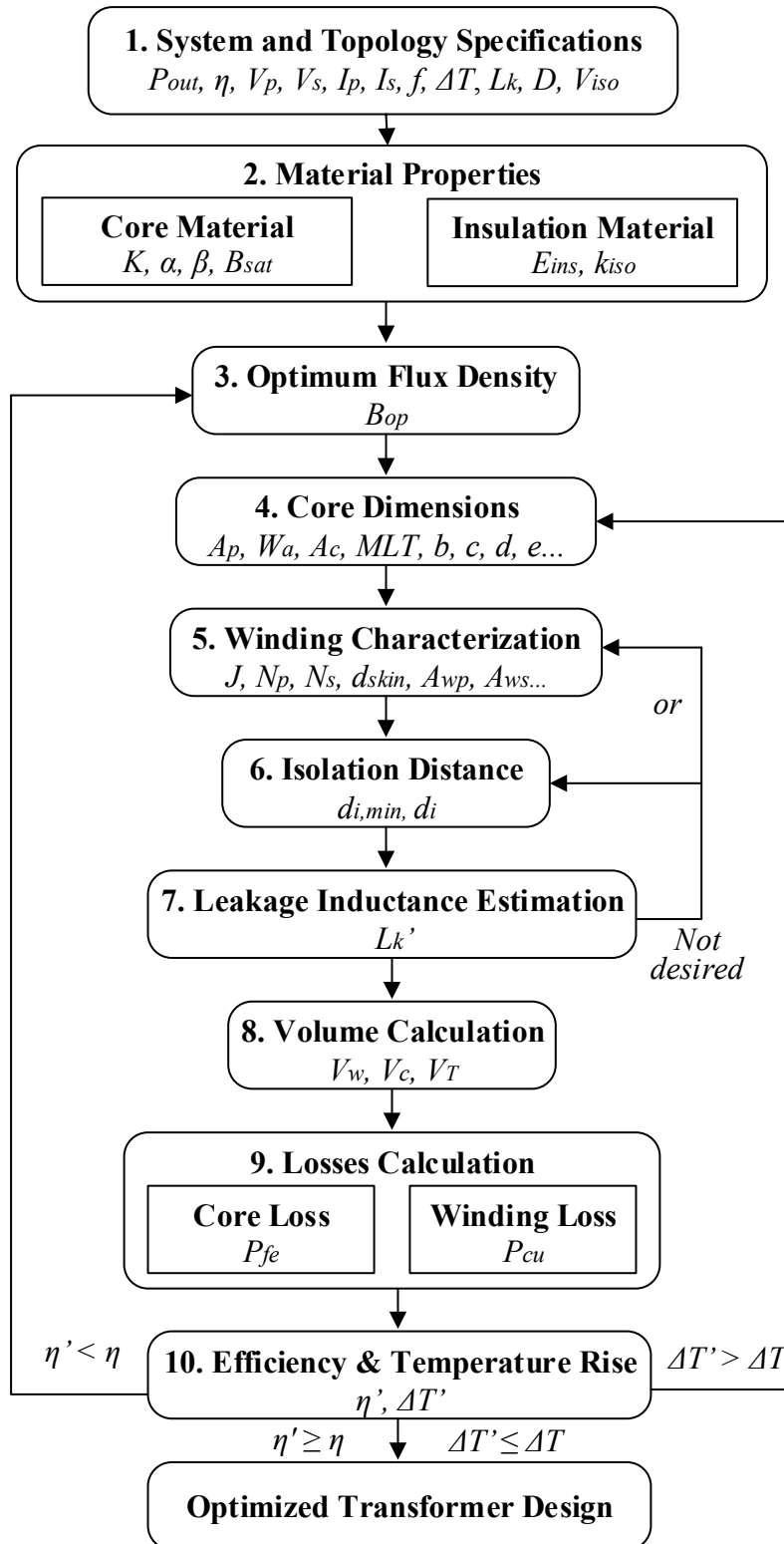
Fig. 4.2. Proposed transformer design flowchart

Step 2. Material Properties

The core material should be selected based on a material characterization as given in Chapter 3. Once the core material is selected, the saturation flux density B_{sat} and the Steinmetz coefficients K, α and β are obtained from the data provided by the manufacturer and introduced in the program. In addition, the insulation material should be selected and two properties have to be specified, the dielectric strength E_{ins}, and the safety margin k_{iso}.

Step 3. Optimum Flux Density

The optimum flux density B_{opt} is now calculated per (4-3). Typical values of the dimensionless coefficients in (4-3) are $k_a = 40$, $k_c = 5.6$, and $k_w = 10$ [2] and are set as fixed parameters. For natural convection, the coefficient of heat transfer h_c is typically 10 W/m² °C; however, this value may change depending of the type of cooling. The window utilization factor k_u can vary from 0.2 to 0.8, being 0.8 a value for a very tight winding and 0.4 a recommended value. The stacking factor k_f relates the effective cross-sectional area of the core with the physical area; its value can be around 0.95 for laminated cores. The waveform factor is $K_v = 4.44$ for a sinusoidal waveform and $K_v = 4$ for a square waveform [2] [4]. If a different voltage waveform is applied, K_v can be derived as explained in [1].

The optimum flux density B_{opt} is compared with the B_{sat}. The calculated value of B_{opt} could be well below B_{sat}; therefore, the designer can choose to increase the operating flux density to a value that does not affect considerably the efficiency but can increase power density. This recalls the tradeoffs between efficiency and volume discussed in Chapter 3.

Step 4. Core Dimensions

The core size is selected based on the area product A_p which is a relationship that can be found in any manufacturer's datasheet and is the product between the window area and the cross-sectional area of a core. The expression to calculate A_p derived in [1] is given by:

$$A_p = \left[\frac{\sqrt{2}\sum VA}{K_v f B_o k_f K_t \sqrt{k_u \Delta T}}\right]^{8/7} \tag{4-4}$$

where K_t is obtained as follows [1]:

$$K_t = \sqrt{\frac{h_c k_a}{\rho_w k_w}} \tag{4-5}$$

With the value of A_p the designer has to identify in a datasheet a core with a larger A_p than the calculated one. If the larger core in the datasheet is not sufficient, stacked cores can be used to complete the desired A_p. The designer can enter the required number of cores and choose if the core arrangement is core or shell type. After the core is selected, the designer can enter the core dimensions and properties from the datasheet. The designer can change the core dimensions in a second iteration if the evaluated temperature rise in step 10 exceeds the desired value.

Step 5. Winding Characterization

Having selected the core, the designer can now select the wire based on the current density which is given by [1]:

$$J_o = K_t \sqrt{\frac{\Delta T}{2k_u}} \cdot \frac{1}{\sqrt[8]{A_p}} \tag{4-6}$$

The value of J_o and the primary and secondary currents are used to calculate the required primary and secondary bare wire areas, respectively. Also, the HF effects on the windings are

considered by using Litz wire; therefore, the skin depth is calculated per (3-15) as explained in Chapter 3. For copper conductors, the skin depth is given by [1]-[3]:

$$\delta = \frac{6.6}{\sqrt{f}} \ (\text{cm}) \tag{4-7}$$

Equation (4-6) gives the maximum radius that should have the strands of the selected Litz wire. The designer can then select the proper gauge for the strands from the manufacturer's datasheet. Then, the required number of strands is calculated with the required total wire area and the selected area of the strands based on the skin depth.

Subsequently, the primary number of turns N_p is calculated from [2]:

$$N_p = \frac{V_p}{K_v k_f A_c B_{opt} f} \tag{4-8}$$

where A_c is the core cross-sectional area. The secondary number of turns N_s is obtained with the voltage transformer ratio. The number of turns is a free parameter in this design methodology since it can be used to adjust the transformer leakage inductance; therefore, in subsequent iterations the designer can change the number of turns. Then, it is necessary to verify that the winding arrangement (i.e., wire size and number of turns) can actually fit in the core window area.

Step 6. Isolation Distance

The isolation voltage and insulation material have been specified in steps 1 and 2. This step calculates the minimum isolation distance between the primary and secondary windings as given by (3-17) and repeated here for completeness [4]:

$$d_{i,min} = \frac{V_{iso}}{k_{iso} E_{ins}} \tag{3-17}$$

The designer can either choose the minimum isolation distance or specify a distance greater than $d_{i,min}$ in order to increase the transformer leakage inductance.

Step 7. Leakage Inductance Estimation

This step estimates the transformer leakage inductance that will result from the design as calculated per (3-18) and repeated here for completeness [1]-[3]:

$$L_k = \mu_o N^2 MLT . \frac{(a + b + 3c)}{3w} \tag{3-18}$$

This equation is only applicable to a shell-type transformer structure. If a core-type structure is desired, 2D or 3D finite element simulations would be required to obtain a more accurate value of leakage inductance. If the desired leakage inductance for maximum power transfer is not achieved, the proposed design allows two parameters to change in order to adjust the leakage inductance, the number of turns or the isolation distance. These parameters can be changed in a subsequent iteration.

Step 8. Volume Calculation

Achieving high power density might be the priority in some cases, but there might be others where the efficiency is more important than power density; hence, this step is useful to provide an estimation of the transformer volume. Then, the designer can evaluate if the result is acceptable or not. The equations to calculate the core V_c and winding V_w volumes are the following [1], [2]:

$$V_c = l_m A_c \tag{4-9}$$

$$V_w = MLT . W_a \tag{4-10}$$

where l_m is the mean length of the core and MLT is the mean length of a turn.

Step 9. Losses Calculation

The total losses are split into core and winding losses. The iGSE is adopted to calculate the core loss. The predetermined equation written in the program is for a three-level excitation waveform as the one shown in Fig. 3.4. This equation can be changed at any time in the MATLAB$^{\circledR}$ code if a different excitation waveform will be applied to the transformer. On the other side, the winding losses are calculated considering the use of Litz wire as explained in Chapter 3. Analytical calculation of losses in Litz wire is also explained in [4].

Step 10. Efficiency and Temperature Rise

Once the losses are calculated, the efficiency is evaluated and compared with the expected efficiency specified in step 1. The designer can discard the results and start a new design process if the efficiency requirement is not fulfilled. The operating flux density can be used as free parameter to start the new design process or the designer can considered the use of a different core material with lower core loss density.

Another important parameter to evaluate is the resulting temperature rise to verify that the predefined temperature rise is not exceeded. A valid assumption to estimate the temperature rise is that the heat produced by the core and winding losses is dissipated uniformly throughout the transformer surface area. Based on that assumption, an equation to estimate the temperature rise ΔT can be written as [5]:

$$\Delta T = \left(\frac{P_T}{A_t}\right)^{0.833} \tag{4-11}$$

where P_T is the total power loss (i.e., core and winding losses) in mW and A_t is the surface area in cm^2 which can be related to the area product as follows [3]:

$$A_t = K_s \sqrt{A_p} \qquad (4\text{-}12)$$

where $K_s = 39.2$ for C cores [3].

If the calculated value of temperature rise exceeds the predefined value, a new set of core dimension parameters should be used. Another option is to perform a thermal analysis in order to implement an appropriate cooling system that also allows a compact transformer design.

Once all the design requirements have been fulfilled, a set of specifications are obtained to fabricate the HF/MF transformer.

4.4 Transformer Design Examples

This section presents transformer design examples realized with the proposed design methodology implemented in the developed MATLAB® program.

4.4.1   Design Example # 1: 200 kVA, 3 kHz, 3800-400 V, shell-type transformer

This transformer design example is based on the case study discussed in Chapter 1 considering the SST topology I described in Chapter 2. The design consists of a shell-type transformer with a power rating of 200 kVA, operating frequency of 3 kHz, and voltage rating of 3.8 kV-400 V. The steps for designing the transformer are described as follows:

Step 1. System and Topology Specifications

$$\text{Rated output power, } P_{out} = 200 \text{ kVA}$$

$$\text{Expected Efficiency, } \eta \geq 98\,\%$$

$$\text{Primary voltage, } V_p = 3800 \text{ V}$$

$$\text{Secondary voltage, } V_s = 400 \text{ V}$$

$$\text{Isolation voltage, } V_{iso} = 95 \text{ kV}$$

$$\text{Primary current, } I_p = 85 \text{ A}$$

$$\text{Secondary current, } I_s = 807.5 \text{ A}$$

$$\text{Frequency, } f = 3 \text{ kHz}$$

$$\text{Ambient temperature, } T_a = 30 \text{ °C}$$

$$\text{Expected temperature rise, } \Delta T = 70 \text{ °C}$$

$$\text{Duty cycle, } D = 0.5$$

$$\text{Waveform factor, } K_v = 4$$

$$\text{Leakage inductance, } L_k = 3.01 \text{ mH}$$

$$\text{Window utilization factor, } k_u = 0.4$$

Step 2. Material Properties

The selected core material is amorphous 2605SA1 whose Steinmetz parameters extracted from [6] are given in Appendix A.1. The selected insulation material is NOMEX with a dielectric strength of 27 kV/mm and a safety margin of 40 % [7].

Step 3. Optimum Flux Density

The resulting optimum flux density calculated per (4-3) is $B_{opt} = 0.3$ T. This value is lower than the saturation flux density $B_{sat} = 1.56$ T and is considered for the design since high efficiency is desired for this particular design.

Step 4. Core Dimensions

The area product calculated per (4-4) is $A_p = 22976 \text{ cm}^4$. The core AMCC-1000 with an

area product of 966 cm^4 is the larger core that can be selected from [6]; therefore, it is required to stack 24 cores in order to fulfill the area product. The desired transformer configuration for this design is shell type which is also specified in the program. The dimensions of the selected core obtained from [6] are introduced in the program.

Step 5. Winding Characterization

The current density calculated per (4-6) is $J = 107.98$ A/cm^2. For this current density, the required primary and secondary bare wire areas are $A_{wp} = 0.7871$ cm^2 and $A_{ws} = 7.4779$ cm^2, respectively. The skin depth at 3 kHz is $\delta = 0.1209$ cm; therefore, the selected Litz wire should have strands with a maximum area of 0.0459 cm^2. The selected strand size is #18 AWG which has an area of 0.8046x10^{-3} cm^2 and a resistivity of 209.5 $\mu\Omega$/cm at 20 °C [3]. The resistivity is adjusted to the maximum operating temperature of 100 °C which results in 275.37 $\mu\Omega$/cm [2]. The minimum primary number of strands is $PS = 96$; thus a custom made Litz wire #18 AWG/100 strands is selected for the design [8]. The same wire size can be used for the secondary winding, but with a total of 1000 strands. After the wire is selected, the number of primary turns is calculated with (4-8) resulting in $N_p = 11$. In order to increase the leakage inductance, $N_p = 18$ is used and the number of secondary turns is $N_s = 2$.

Step 6. Isolation Distance

The insulation material has been specified in step 1, then the minimum isolation distance between windings calculated by (3-17) is $d_{i,min} = 8.8$ mm. This is a free parameter that will be adjusted in order to meet the leakage inductance requirement in the next step.

Step 7. Leakage Inductance Estimation

The estimation of the leakage inductance per (3-18) gives $L_k = 1.8$ mH. After some iterations, the selected isolation distance is $d_i = 35$ mm which leads to $L_k = 3.1$ mH.

Step 8. Volume Calculation

The core volume calculated by (4-9) is $V_c = 47.14$ dm^3 and the winding volume using (4-10) is $V_w = 36.76$ dm^3; thus, the total transformer volume is $V_T = 83.90$ cm^3.

Step 9. Losses Calculation

For the selected parameters, the core loss is $P_{fe} = 2.281$ kW and the winding loss is $P_{cu} = 0.313$ kW; thus, the total transformer loss is $P_T = 2.594$ kW.

Step 10. Efficiency and Temperature Rise

As a result, the calculated transformer efficiency is $\eta = 98.7$ % which meets the desired efficiency specified in step 1. The temperature rise estimated per (4-11) results in $\Delta T = 88$ °C considering natural convection. This value is greater than the expected temperature rise previously specified; therefore, a proper cooling system must be incorporated to the design in order to meet this requirement [4]. Otherwise, the designer should select a larger core.

The efficiency and size of the transformer have been optimized with the selected parameters. In addition, the required inductance for maximum power transfer with the DAB has been integrated into the transformer leakage inductance which eliminates the need for an external inductor to meet the desired inductance. The design as obtained from the MATLAB program is presented in the Appendix B.2.

4.4.2 Design Example # 2: 20 kVA, 3 kHz, 3800-400 V, core-type transformer

This is a design example of a core-type transformer with a power rating of 20 kVA, operating frequency of 3 kHz, and voltage rating of 3800-400 V.

Step 1. System and Topology Specifications

$$\text{Rated output power, } P_{out} = 20 \text{ kVA}$$

$$\text{Expected Efficiency, } \eta \geq 98 \text{ \%}$$

$$\text{Primary voltage, } V_p = 3800 \text{ V}$$

$$\text{Secondary voltage, } V_s = 400 \text{ V}$$

$$\text{Isolation voltage, } V_{iso} = 65 \text{ kV}$$

$$\text{Primary current, } I_p = 9 \text{ A}$$

$$\text{Secondary current, } I_s = 85 \text{ A}$$

$$\text{Frequency, } f = 3 \text{ kHz}$$

$$\text{Ambient temperature, } T_a = 30 \text{ °C}$$

$$\text{Expected temperature rise, } \Delta T = 65 \text{ °C}$$

$$\text{Duty cycle, } D = 0.5$$

$$\text{Waveform factor, } K_v = 4$$

$$\text{Leakage inductance, } L_k = 60.2 \text{ mH}$$

$$\text{Window utilization factor, } k_u = 0.4$$

Step 2. Material Properties

From the magnetic materials discussed in Chapter 3, amorphous 2605SA1 is selected because its cost is lower than the nanocrystalline. The selected insulation material is NOMEX with a dielectric strength of 27 kV/mm and a safety margin of 40 % [7].

Step 3. Optimum Flux Density

The calculated optimum flux density is $B_{opt} = 0.4$ T.

Step 4. Core Dimensions

The area product calculated for the optimum condition is $A_p = 1234.9$ cm^4. Therefore, two (2) stacked cores AMCC-1000 with area product of 966 cm^4 are needed. The desired transformer configuration for this design is core type which leads to a higher leakage inductance. The resulting area product is $A_p = 1932$ cm^4.

Step 5. Winding Characterization

The wire is selected based on the current density calculated per (4-6) which gives $J = 168.82$ A/cm^2. The minimum primary and secondary bare wire areas are $A_{wp} = 0.0533$ cm^2 and $A_{ws} = 0.4857$ cm^2, respectively. The skin depth at 3 kHz is $\delta = 0.1209$ cm and the maximum allowable area for the strands is 0.0459 cm^2; therefore, the selected Litz wire is #30 AWG/110 strands which is equivalent to a #10 AWG wire. The area of each strand is $0.5067\text{x}10^{-3}$ cm^2 and the resistivity at 20 °C is 3402 μΩ/cm at 20 °C [9]. The resistivity is adjusted according to the maximum operating temperature of 95 °C (= 30 + 65 °C) which results in 4404.7 μΩ/cm [2]. The selected wire is also used for the secondary winding with ten of them

in parallel which makes a total of 1100 strands. The number of turns in the primary winding is $N_p = 181$ and in the secondary is $N_s = 20$.

Step 6. Isolation Distance

The minimum isolation distance between windings calculated per (3-17) for an isolation level of 65 kV is $d_{i,min} = 6$ mm. An extra safety margin is considered; therefore, $d_i = 8$ mm is specified isolation distance.

Step 7. Leakage Inductance Estimation

This example is for a core-type transformer structure; therefore, the estimation of the leakage inductance using (3-18) is not applicable. However, it is known that the core-type structure can result in a much larger leakage inductance than the shell-type structure.

Step 8. Volume Calculation

The estimated core volume is $V_c = 1.96$ dm^3 and the winding volume is $V_w = 2.40$ dm^3. The total transformer volume is $V_T = 4.36$ dm^3.

Step 9. Losses Calculation

The operation at the specified conditions leads to a core loss of $P_{fe} = 197.18$ W and winding loss of $P_{cu} = 64.22$ W; thus, the total transformer loss is $P_T = 261.4$ W.

Step 10. Efficiency and Temperature Rise

As a result, the calculated transformer efficiency is $\eta = 98.71$ %. The temperature rise

estimated per (4-11) results in $\Delta T = 65.58\,°C$ for natural convection compared with $\Delta T = 65\,°C$ specified in step 1. Therefore, the design has been successfully optimized in efficiency and size.

4.4.3 Design Example # 3: 2 kVA, 20 kHz, 600-60 V, shell-type transformer

It is desired to build a transformer with a power rating of 2 kVA, operating frequency of 20 kHz, and voltage rating of 600-60 V as a scaled-down prototype used for testing new power converter topologies for SSTs [10].

Step 1. System and Topology Specifications

$$\text{Rated output power, } P_{out} = 2 \text{ kVA}$$

$$\text{Expected Efficiency, } \eta \geq 98\,\%$$

$$\text{Primary voltage, } V_p = 600 \text{ V}$$

$$\text{Secondary voltage, } V_s = 60 \text{ V}$$

$$\text{Isolation voltage, } V_{iso} = 1.0 \text{ kV}$$

$$\text{Primary current, } I_p = 4 \text{ A}$$

$$\text{Secondary current, } I_s = 40 \text{ A}$$

$$\text{Frequency, } f = 20 \text{ kHz}$$

$$\text{Ambient temperature, } T_a = 25\,°C$$

$$\text{Expected temperature rise, } \Delta T = 60\,°C$$

$$\text{Duty cycle, } D = 0.5$$

$$\text{Waveform factor, } K_v = 4$$

$$\text{Leakage inductance, } L_k = 1.1 \text{ mH}$$

$$\text{Window utilization factor, } k_u = 0.4$$

70

Step 2. Material Properties

Amorphous 2605SA1 core is selected due to its lower cost and greater availability compared with nanocrystalline core. The selected insulation material is MICA with a dielectric strength of 15 kV/mm and a safety margin of 40 % [4].

Step 3. Optimum Flux Density

The calculated optimum flux density is $B_{opt} = 0.144$ T. The specified operating flux density is then 0.15 T.

Step 4. Core Dimensions

The resulting area product is $A_p = 32.83$ cm^4; therefore, the core AMCC-50 with $A_p = 45.9$ cm^4 is selected for this design [6]. Since it is desired to build the transformer with a shell-type configuration, two sets of C-cores are used as shown in Fig. 4.3. The resulting area product is then $A_p = 184.8$ cm^4.

Step 5. Winding Characterization

The calculated current density according to the previous specifications is $J = 2178.5$ A/cm^2. Then, the primary and secondary bare wire areas are $A_{wp} = 0.0184$ cm^2 and $A_{ws} = 0.1839$ cm^2, respectively. The maximum allowable area that is used to choose the strands size is 0.0069 cm^2 according to a skin depth of $\delta = 0.0468$ cm at 20 kHz. The Litz wire #36 AWG/259 equivalent to #12 AWG shown in Fig. 4.4 was selected because it meets the requirements and was available in stock for a single purchase. The strands of the selected Litz wire have an area of 0.1266×10^{-3} cm^2 and a resistivity at 20 °C of 13608 $\mu\Omega$/cm. The selected

wire is also used for the secondary winding with six of them in parallel. The number of turns in the primary winding is $N_p = 80$ and in the secondary is $N_s = 8$.

Step 6. Isolation Distance

The minimum isolation distance between windings for an isolation level of 1 kV is $d_{i,min} = 0.17$ mm, thus 0.20 mm is considered.

Fig. 4.3. Two sets of C-cores AMCC-50 in a shell-type configuration

Fig. 4.4. Litz wire 259/36 for transformer prototypes

Step 7. Leakage Inductance Estimation

The estimated leakage inductance is 1.9 mH, therefore, there is no need to adjust the isolation distance or number of turns to meet the leakage inductance requirement.

Step 8. Volume Calculation

The total transformer volume is $V_T = 0.71$ dm^3.

Step 9. Losses Calculation

The resulting core loss is $P_{fe} = 101.91$ W and winding loss is $P_{cu} = 4.42$ W; thus, the total transformer loss is $P_T = 106.33$ W.

Step 10. Efficiency and Temperature Rise

As a result, the transformer efficiency is $\eta = 95\,\%$ and the temperature rise is $\Delta T = 82.4\,°C$ for natural convection. The experimental prototype is shown in Fig. 4.5 and the main specifications are listed in Table 4.2. The desired efficiency was not achieved because it was not possible to build the transformer with the optimum parameters since it was necessary to consider low cost materials and only the cores available in stock in order to get a shorter lead time. Otherwise, the designer should select the proper core and wire according to the optimum conditions.

Fig. 4.5. Transformer prototype #1

Table 4.1. Main specifications of the transformer prototype #1

Power rating	2 kVA
Primary/secondary voltage	600-60 V
Frequency	20 kHz
Core Material	AMCC-50 Metglas 2605SA1
Wire type	259/36 served Litz wire
Isolation distance	0.2 mm
Number of winding turns	80 primary/ 8 secondary
Leakage inductance	~ 1.86 mH
Efficiency	~ 95 %
Temperature rise	~ 82 °C

4.4.4 Design Example # 4: 2 kVA, 20 kHz, 600-60 V, core-type transformer

The same specifications from the example #3 are considered for a second transformer prototype built in a core-type configuration as shown in Fig. 4.6. The main results from the design are listed in Table 4.3. The core AMCC-80 was used instead of the AMCC-50 in order to meet the desired area product for optimum conditions. The required isolation distance between windings is 0.2 mm for an isolation level of 1 kV. A larger leakage inductance is obtained with this transformer structure when compared with the shell-type structure. The expected efficiency was 98% and a temperature rise of 60 ℃; however, the exact parameters obtained for optimum conditions where not used due to limitation on materials availability.

Fig. 4.6. Transformer prototype #2 in a core-type configuration

Table 4.2. Main specifications of the transformer prototype #2

Power rating	2 kVA
Primary/secondary voltage	600-60 V
Frequency	20 kHz
Core Material	AMCC-80 Metglas 2605SA1
Wire type	259/36 served Litz wire
Isolation distance	0.2 mm
Number of winding turns	100 primary/ 10 secondary
Leakage inductance	~ 2.87 mH
Efficiency	~ 97 %
Temperature rise	~ 79 °C

4.5 Conclusions

Each step of the proposed transformer design methodology and the principles for the optimization criteria were described in this chapter. The design methodology is oriented towards obtaining the highest efficiency by calculating the optimum flux density at which the core losses and the copper losses are equal. However, if the design is mainly driven by power density and not the efficiency, then the flux density can be modified according to the desired outcome. In addition, the design methodology includes the estimation of the leakage inductance for shell-type transformer configurations. This design methodology was implemented in MATLAB® as an interactive tool for designing single-phase HF/MF transformers. The MATLAB® program has

been verified with design examples and the fabrication of two scaled-down prototypes used for

testing of power converter topologies for SSTs.

4.6 References

[1]   W. G. Hurley, W.H. Wölfle, Transformers and Inductors for Power Electronics: Theory, Design and Applications, 1st ed., Wiley, 2013.

[2]   W.G. Hurley, W. H. Wöfle, J. G. Breslin, "Optimized transformer design: Inclusive of high-frequency effects," *IEEE Transactions on Power Electronics*, vol. 13, no. 4, pp. 651-659, July 1998.

[3]   C. William, T. McLyman, Transformer and Inductor Design Handbook, 4th ed., Taylor & Francis Group, 2011.

[4]   G. Ortiz, J. Biela, J. W. Kolar, "Optimized design of medium frequency transformers with high isolation requirements," in *Proceeding of the 36th IEEE Industrial Electronics Society Conference*, IECON 2010, pp. 631-638, Nov. 2010.

[5]   "Estimating temperature rise of transformers," [Online]. Available: http://www.tscinternational.com/tech12.pdf [Accessed May 2015].

[6]   Metglas Powerlite, "Technical bulletin," [Online]. Available: http://www.elnamagnetics.com/wp-content/uploads/catalogs/metglas/powerlite.pdf [Accessed May 2015]

[7]   [Online]. Available: http://www.dupont.com/content/dam/assets/products-and-services/electronic-electrical-materials/assets/DPP_Nomex410_K20612-1.pdf [Accessed April 2015]

[8]   Cooner Wire, "Type 8 rectangular litz," [Online]. Available: http://www.coonerwire.com/type-8/ [Accessed May 2015]

[9]   New England Wire Technologies, "Round litz wire," [Online]. Available: http://www.newenglandwire.com/products/litz-wire-and-formed-cables/round [Accessed May 2015].

[10] R. J. Garcia Montoya, A. Mallela, J. C. Balda, "An evaluation of selected solid-state transformer topologies for electric distribution systems," in *Proceedings of the IEEE 30th Applied Power Electronics Conference and Exposition*, APEC 2015, pp. 1022-1029, March 2015.

HIGH-FREQUENCY TRANSFORMER DESIGN TOOL

This appendix presents the proposed high-frequency transformer design tool implemented

in MATLAB®. This tool allows to design a single-phase high- or medium-frequency transformer

with either core- or shell-type structure following the design flowchart described in Chapter 4.

```matlab
%% HIGH-FREQUENCY TRANSFORMER DESIGN TOOL
disp('===== HIGH-FREQUENCY TRANSFORMER DESIGN TOOL =====')
disp('WITH THIS TOOL YOU WILL BE DESIGNING A SINGLE-PHASE HIGH- OR MEDIUM-
FREQUENCY TRANSFORMER')
disp('SHELL-TYPE OR CORE-TYPE STRUCTURE')
disp('FOR MORE INFORMATION REFER TO THE THESIS:')
disp(' ')
disp('"HIGH-FREQUENCY TRANSFORMER DESIGN FOR SOLID-STATE TRANSFORMERS IN
ELECTRIC POWER DISTRIBUTION SYSTEMS"')
disp('BY RODERICK J. GARCIA M.')
disp(' ')
disp('**To interrupt this program at any time enter "ctrl+c"**')
disp(' ')

%% STEP 1. SYSTEM AND TOPOLOGY SPECIFICATIONS
disp('===== STEP 1. SYSTEM AND TOPOLOGY SPECIFICATIONS =====')
disp(' ')
prompt='Enter output power (VA): ';
Pout=input(prompt);    %Output power in VA
prompt='Enter expected efficiency (%): ';
n=input(prompt)/100;%Desired efficiency
Pin=Pout/n;          %Input Power (VA)
SVA=Pin+Pout;        %Sum of input power and output power
prompt='Enter primary voltage (V): ';
Vp=input(prompt);    %Primary voltage (V)
prompt='Enter secondary voltage (V): ';
Vs=input(prompt);    %Secondary voltage (V)
prompt='Enter the isolation voltage level "Viso"(kV): ';
Viso=input(prompt); %Isolation voltage level (kV)
prompt='Enter primary current (A): ';
Ip=input(prompt);    %Primary current (A)
prompt='Enter secondary current (A): ';
Is=input(prompt);    %Secondary Current (A)
prompt='Enter operating frequency (Hz): ';
f=input(prompt);     %Frequency (Hz)
T=1/f;               %Period (s)
prompt='Enter ambient temperature (C): ';
Ta=input(prompt);     %Ambient temperature (Hz)
prompt='Enter expected temperature rise (C): ';
DT=input(prompt);    %Temperature rise (C)
Tmax=Ta+DT; %Maximum temperature
```

```matlab
prompt='Enter duty cycle (between 0 and 1): ';
D=input(prompt);     %Duty Cycle
prompt='Enter waveform factor Kv (Ex. Square wave Kv=4 / Sinusoidal Kv=4.44):
';
Kv=input(prompt);    %Waveform factor
prompt='Enter desired leakage inductance in (H): ';
Lk=input(prompt);   %Desired leakage inductance for maximum power transfer (H)
prompt='Enter window utilization factor (between 0 and 1)(Ex. 0.4): ';
ku=input(prompt);    %Window utilization factor
disp(' ')
%% Coefficients and dimensional parameters. Typical values (Ref.[1] pag. 61)
hc=10;               %Coefficient of heat transfer 10W/m^2C for natural
convection. Up to 30W/m^2C
ka=40;               %Dimensionless Quantity (Ref.[1] pag. 61)
kw=10;               %Dimensionless Quantity (Ref.[1] pag. 61)
kc=5.6;              %Dimensionless Quantity (Ref.[1] pag. 61)
kf=0.95;             %Core stacking factor
phiw=1.72e-8;        %initial wire resistivity for flux density and area
product calculations (ohm*m)
Tcoef=0.00393;       %Temperature coefficient of resistivity @20 C per degree
C for Copper wires
%% STEP 2. MATERIAL PROPERTIES
disp('===== STEP 2. MATERIAL PROPERTIES =====')
disp(' ')
disp('Core Material')
prompt='Enter selected core material: 1 for amorphous, 2 for ferrite, 3 for
nanocrystalline, or 4 for other: ';
material=input(prompt);
if (material==1)
    Kc=1.3617;           %Coefficient of the Steinmetz equation in (W/m3)
    alpha=1.51;          %Coefficient of the Steinmetz equation
    beta=1.74;           %Coefficient of the Steinmetz equation
    Bsat=1.56;           %Saturation flux density (T)
elseif (material==2)
    Kc=17.1;             %Coefficient of the Steinmetz equation in (W/m3)
    alpha=1.46;          %Coefficient of the Steinmetz equation
    beta=2.75;           %Coefficient of the Steinmetz equation
    Bsat=0.47;           %Saturation flux density (T)
elseif (material==3)
    Kc=2.3;              %Coefficient of the Steinmetz equation in (W/m3)
    alpha=1.32;          %Coefficient of the Steinmetz equation
    beta=2.12;           %Coefficient of the Steinmetz equation
    Bsat=1.2;            %Saturation flux density (T)
elseif (material==4)
    prompt='Enter Steinmetz coefficient "Kc" in (W/m^3): ';
    Kc=input(prompt);
    prompt='Enter Steinmetz coefficient "alpha": ';
    alpha=input(prompt);
    prompt='Enter Steinmetz coefficient "beta": ';
    beta=input(prompt);
    prompt='Enter saturation flux density (Bsat) in (T): ';
    Bsat=input(prompt);
end
disp(' ')
disp('Insulation Material')
prompt='Enter dielectric strength of selected insulation material "Eins" in
(kV/mm): ';
```

```matlab
Eins=input(prompt);    %Dielectric strength of the insulation material in
(kV/mm)
prompt='Enter a safety margin for isolation requirement "kiso"(Ex. 0.4): ';
kiso=input(prompt);              %Safety margin parameter for isolation
requirement
disp(' ')

%% STEP 3. OPTIMUM FLUX DENSITY
disp('===== STEP 3. OPTIMUM FLUX DENSITY =====')
disp(' ')
Bop=(((hc*ka*DT)^(2/3))./((1.5874).*((phiw*kw*ku)^(1/12)).*(kc*Kc.*f.^alpha).
^(7/12))).*((Kv.*f.*kf*ku./SVA).^(1/6)) %Tesla (T) (Ref.[1] pag. 126)
disp('This is the calculated optimum flux density. Bear in mind the tradeoff
between efficiency and volume.')
disp('If the flux density is increased, the volume can be reduced, but also
the efficiency gets reduced')
disp('**Always consider Bop < Bsat')
disp(' ')
prompt='If Bop is the desired flux density, enter Y, if this is not the
desired flux density, enter N: ';
desired=input(prompt,'s');
if (strcmp(desired,'Y') || strcmp(desired,'y')) %if user enters yes
    Bop=Bop; %calculated flux density will be used
elseif (strcmp(desired,'N') || strcmp(desired,'n')) %if user enters no
    prompt='Enter the desired flux density in (T): ';
    Bop=input(prompt); %Introduce a different value of flux density when the
optimum is not desired
else error('Program exit') %if user does not enter a proper choice, exit
end
DB=2*Bop;  %Peak to Peak Flux Density
disp(' ')

%% STEP 4. CORE DIMENSIONS
disp('===== STEP 4. CORE DIMENSIONS =====')
disp(' ')
disp('Area Product:')
Kt=(hc*ka/(phiw*kw))^0.5;   %48.2x10^3 (Ref.[1] pag. 61)
Ap=(((sqrt(2))*SVA./(Kv.*f.*Bop*kf*Kt.*((ku*DT).^(0.5)))).^(8/7))*1e8
%(cm^4)(Ref.[1] pag. 125)
disp('Based on Ap, select a core from a data sheet whose area product is
larger than the calculated value')
disp('Consider stacked cores if the larger area product in the data sheet is
not sufficient')
disp(' ')
prompt='Enter the selected core series number (Ex. AMCC-100): ';
Core=input(prompt,'s');   %core number
prompt='Enter the number of stacked cores needed to achieve optimum Ap. If
stacked cores are not needed, enter 1: ';
Nc=input(prompt);   %number of cores needed to achieve the optimum Ap
prompt='If a Shell-type transformer structure is considered, enter "S" If a
Core-type is considered, enter "C": ';
cont=input(prompt, 's');
if (strcmp(cont,'S') || strcmp(cont,'s')) %if user enters shell-type
        shell_factor = 2; %this will be used to double the mean length and
the mass
elseif (strcmp(cont,'C') || strcmp(cont,'c')) %if user enters core-type
```

```matlab
        shell_factor = 1; %this will be multiplied by the mean length and
mass and they will not be doubled
else error('Program exit') %if user does not enter a proper choice
end
disp('Now you have to enter the core dimensions from data sheet. See Metglas
data sheet for label references')
prompt='Enter the total width "d"(cm): ';
d=input(prompt)*Nc; %core width (cm)
prompt='Enter the height of the window area "c"  (cm): ';
c=input(prompt);  %height of window area (cm)
prompt='Enter height of the core "f" (cm): ';
f1=input(prompt);   %height of core (cm)
prompt='Enter the length of the window area "b" (cm): ';
b=input(prompt);  %length of the window area (cm)
prompt='Enter the length of the core "e" (cm): ';
e=input(prompt);    %length of the core (cm)
l=0.5*(e-b);     %length of cross sectional area (cm)
prompt='Enter the mean length of the core "lm" (cm): ';
lm=input(prompt);   %mean length of the core (x2 if shell type)(cm)
prompt='Enter the cross sectional area of the core "Ac" (cm^2): ';
Ac=input(prompt)*shell_factor*Nc; %cross sectional area of core (cm^2)
(shell_fator will be 2 if shell type, otherwise it will be 1)
Wa = b*c*shell_factor;      %Window Area (cm^2)
prompt='Enter the mass of the core (g): ';
m = input(prompt)*Nc*shell_factor;  %mass of core (shell_fator will be 2 if
shell type, otherwise is will be 1)(grams)
prompt='Enter the density of the core (g/cm^3): ';
density = input(prompt);    %(g/cm^3)
V=m/density;         %core volume from datasheet
disp('This is the real area product of the core:')
Ap = Wa*Ac        %Area product (cm^4)
Apm = Ap/(100^4);  %Area product (m^4)
disp(' ')


%% STEP 5. WINDING CHARACTERIZATION
disp('===== STEP 5. WINDING CHARACTERIZATION =====')
disp(' ')
disp('Calculated current density J (A/cm^2)')
J = (((hc*ka*DT)/(2*phiw*kw*ku))^(1/2))*(1/(Apm^(1/8)))/(100^2) %Current
Density  (A/cm^2) (Ref.[1] pag. 125)
%% Selection of wire dimension (considering skin effect due to high-frequency
operation)
disp('Required total wire area based on current density, and primary and
secondary currents (cm^2)')
Awp = Ip/J                 % Required primary bare wire area (cm^2)
Aws = Is/J                 % Required secondary bare wire area (cm^2)
disp('Skin depth (cm):')
skin = 6.62/(sqrt(f))       % Skin depth (cm)
disp('Maximum wire diameter (single strand) (cm):')
dskin = 2*skin              % bare conductor diameter  (cm)
disp('Maximum wire area (single strand) (cm^2):')
Askin = pi*skin^2           % bare conductor area (cm^2)
prompt='Enter area of selected strand size based on Askin or dskin (cm^2): ';
Aw = input(prompt);         % Cross sectional area of selected wire  (cm^2)
prompt='Enter conductor resistivity @20 C(uOhm/cm): ';
rho=input(prompt);          % Resistivity of selected conductor @20
C(uOhm/cm)
```

```matlab
disp('Resistivity of the selected conductor at maximum operating temperature
(uOhm/cm): ')
rhomax=rho*(1+Tcoef*(Tmax-20))% Resistivity at maximum operating temperature
(uOhm/cm)
disp('Minimum number of primary strands "PS"')
PS = round(Awp/Aw)            % Required number of primary strands
prompt='If PS is the desired number of primary strands, enter Y. If not,
enter N: ';
desired=input(prompt,'s');
if (strcmp(desired,'Y') || strcmp(desired,'y')) %if user enters yes
    PS=PS;                    %calculated PS will be used
elseif (strcmp(desired,'N') || strcmp(desired,'n')) %if user enters no
    prompt='Enter the desired PS: ';
    PS=input(prompt);         %Introduce a different value of PS
else error('Program exit')  %if user does not enter a proper choice, exit
end
disp('Minimum number of secondary strands "SS"')
SS = round(Aws/Aw)            % Required number of secondary strands
prompt='If SS is the desired number of secondary strands, enter Y. If not,
enter N: ';
desired=input(prompt,'s');
if (strcmp(desired,'Y') || strcmp(desired,'y')) %if user enters yes
    SS=SS;                    %calculated SS will be used
elseif (strcmp(desired,'N') || strcmp(desired,'n')) %if user enters no
    prompt='Enter the desired SS: ';
    SS=input(prompt);         %Introduce a different value of SS
else error('Program exit')  %if user does not enter a proper choice, exit
end
%% Number of primary and secondary turns
disp('Number of primary turns "Np":')
Np = Vp./(Kv.*Bop.*kf*Ac*(10^-4)*f);     %Number of turns primary (Ref.[1]
pag. 128)
Np=ceil(Np)
disp('The number of turns is a free parameter that can adjust the leakage
inductance')
prompt='If Np is the desired number of primary turns, enter Y. If not, enter
N: ';
desired=input(prompt,'s');
if (strcmp(desired,'Y') || strcmp(desired,'y')) %if user enters yes
    Np=Np;                    %calculated Np will be used
elseif (strcmp(desired,'N') || strcmp(desired,'n')) %if user enters no
    prompt='Enter the desired Np: ';
    Np=input(prompt);         %Introduce a different value of Np
else error('Program exit')  %if user does not enter a proper choice, exit
end

disp('Number of secondary turns "Ns":')
Ns = Np*(Vs/Vp)            %Number of secondary turns
prompt='If Ns is the desired number of secondary turns, enter Y. If not,
enter N: ';
desired=input(prompt,'s');
if (strcmp(desired,'Y') || strcmp(desired,'y')) %if user enters yes
    Ns=Ns;                    %calculated Np will be used
elseif (strcmp(desired,'N') || strcmp(desired,'n')) %if user enters no
    prompt='Enter the desired Ns: ';
    Ns=input(prompt);         %Introduce a different value of Ns
else error('Program exit')  %if user does not enter a proper choice, exit
```

83

```matlab
    end

disp('Mean Length Turn (MLT):')
MLT = (2*d)+2*(shell_factor*l)+(b*0.8)*(2+pi)     %Mean Length Per turn (cm)
(Ref. [2] Eq. 4-23, Ref. [3])
disp('**Verify that the selected winding arrangement can actually fit in the
core window area**')
disp(' ')

%% STEP 6. ISOLATION DISTANCE
disp('===== STEP 6. ISOLATION DISTANCE =====')
disp(' ')
disp('This is the minimum isolation distance between primary and secondary
windings based')
disp('on the isolation level and insulation material (mm): ')
dimin=Viso/(kiso*Eins)  %Minimum isolation distance between primary and
secondary windings (mm) (Ref. [4])
disp('The isolation distance dimin could be increased in order to adjust the
leakage inductance')
disp('**di>dimin')
prompt='If dimin is the desired isolation distance, enter Y. If not, enter N:
';
desired=input(prompt,'s');
if (strcmp(desired,'Y') || strcmp(desired,'y')) %if user enters yes
    dimin=dimin; %calculated Np will be used
elseif (strcmp(desired,'N') || strcmp(desired,'n')) %if user enters no
    prompt='Enter the desired di: ';
    dimin=input(prompt); %Introduce a different value of di
else error('Program exit') %if user does not enter a proper choice, exit
end
disp(' ')

%% STEP 7. LEAKAGE INDUCTANCE ESTIMATION
disp('===== STEP 7. LEAKAGE INDUCTANCE ESTIMATION =====')
disp(' ')
disp('This estimation is only applicable to a shell-type structure. If a
Core-type structure was selected,')
disp('a leakage inductance estimation would require 2D or 3D Finite Element
simulations')
disp('Calculated leakage inductance (H):')
Lkp=(4*pi*10^-7).*(Np^2).*MLT*(c+3*(dimin*10^-1))*(10^-2)/(3*b) %Primary
leakage inductance (H)
disp(' ')
if (Lk>Lkp)
    disp('The estimated leakage inductance is lower than the desired value
previously entered');
    prompt='To continue with this leakage inductance enter Y. To reject this
design and start over enter N: ';
    continueprocess=input(prompt,'s');
    if (strcmp(continueprocess,'Y') || strcmp(continueprocess,'y')) %if user
enters yes
        Lkp=Lkp;
    else
        disp('If this value is not desired, it could be adjusted in a second
iteration by modifying the number of')
        disp('primary turns or increasing the isolation distance.')
```

```matlab
        error('Program exit') %if user enters no or if the user enters a
value that is not valid
    end
else
    Lkp=Lkp; %if the Lkp is greater or equal than Lk, continue
end
disp(' ')


%% STEP 8. VOLUMEN CALCULATION
disp('===== STEP 8. VOLUMEN CALCULATION =====')
disp(' ')
disp('Calculated volume of windings (cm^3)')
Vw=MLT*Wa       %Volume of the windings cm^3
disp('Calculated volume of core (cm^3)')
Vc=lm*Ac        %Volume of the core cm^3
Vt=Vw+Vc;       %total volume in cm^3
disp('Calculated total volume (dm^3)')
Vtd=(1e-3).*Vt   %in dm^3
Vtm=(1e-6)*Vt;   %in m^3
disp(' ')


%% STEP 9. LOSSES CALCULATION
disp('===== STEP 9. LOSSES CALCULATION =====')
disp(' ')
disp('Core loss using the iGSE')
disp('in (W/m^3):')
ki = Kc/(2^(beta-1)*pi^(alpha-1)*(1.1044+(6.8244/(alpha+1.354))));
%Approximation of ki iGSE (Ref.[1] pag. 204)
Pvi = ki*(DB^(beta-alpha))*(1/T)*(2*DB^alpha*(D*T)^(1-alpha)) %Loss per unit
volume (iGSE) (W/m3)(Ref.[1] pag. 204)
disp('in (W):')
Pfei = Vtm*Pvi              %Core losses (iGSE) (W)
disp(' ')
disp('Winding loss (W):')
rhop = rhomax/PS;            %Primary Resistance per cm (uOhm/cm)
rhos = rhomax/SS;            %Secondary resistance per cm (uOhm/cm)
RP = rhop*Np*MLT*(10^-6);   %Total Primary Resistance (Ohm)
RS = rhos*Ns*MLT*(10^-6);   %Total Secondary Resistance (Ohm)
Pcup = RP*(Ip^2);           %Primary Copper Losses(W)
Pcus = RS*(Is^2);           %Secondary Copper Losses (W)
Pcu = Pcup + Pcus           %Total Copper Losses (W)
disp(' ')
disp('Total loss (W):')
Pt = Pfei + Pcu         %Total loss with iGSE(W)
disp(' ')


%% STEP 10. EFFICIENCY & TEMPERATURE RISE
disp('===== STEP 10. EFFICIENCY & TEMPERATURE RISE =====')
disp(' ')
disp('Calculated efficiency: ')
Effi = Pout/(Pout + Pt)      %Efficiency
disp('The efficiency could be increased in a second iteration by reducing the
operating flux density in Step 3.')
disp('If the optimum flux density has been used and the obtained efficiency
is not desired, consider using a')
disp('different core material.')
```

```matlab
disp(' ')
disp('Temperature rise estimation: ')
Ks=39.2;                %For C core Table 5-4 Ref. [2]
disp('Surface area (cm^2): ')
At=Ks*(Ap)^0.5      %Surface area (cm^2)Eq. 5-30 Ref. [2]
Pdis=Pt/At;         %power dissipated per unit area (W/cm^2)Eq. 6-17 Ref. [2]
DT1=450*(Pdis)^0.826;  %Temperature rise (C) Eq. 6-19 Ref. [2]
disp('Estimated temperature rise (Celsius): ')
DT2=(Pt*1000/At)^0.833 %Temperature rise (C) Ref. [5]
%check to see if calculated temperature rise exceeds the desired value
previously entered
if (DT2>DT)
    disp('The calculated temperature rise exceeds the desired value
previously entered');
    prompt='To continue with this temperature rise enter Y. To reject this
and start the design process over enter N: ';
    continueprocess=input(prompt,'s');
    if (strcmp(continueprocess,'Y') || strcmp(continueprocess,'y')) %if user
enters yes
        DT2=DT2;
    else
        disp('In order to decrease the temperature, select a larger core');
        error('Program exit') %if user enters no or if the user enters a
value that is not valid
    end
else
    DT2=DT2; %if the DT (desired temperature rise) is greater or equal than
DT2, continue
end
disp(' ')

%% SUMMARY OF THE RESULTS
disp('===== SUMMARY OF THE RESULTS =====')
disp(' ')
disp(sprintf('Pout=''%d''VA Rated power',Pout));
disp(sprintf('Vp=''%d''V Primary voltage',Vp));
disp(sprintf('Vs=''%d''V Secondary voltage',Vs));
disp(sprintf('f=''%d''Hz Frequency',f));
if (material == 1)
    disp('Core material = Amorphous')
elseif (material == 2)
    disp('Core material = Ferrite')
elseif (material == 3)
    disp('Core material = Nanocrystalline')
elseif (material == 4)
    disp('Core material = other')
end
disp(sprintf('Core=''%s''Core number',Core));
disp(sprintf('B=''%0.2d''T Flux density',Bop));
disp(sprintf('Np=''%d''Primary turns',Np));
disp(sprintf('Ns=''%d''Secondary turns',Ns));
disp(sprintf('Awp=''%0.4d''cm^2 Required total primary wire area',Awp));
disp(sprintf('Aws=''%0.4d''cm^2 Required total secondary wire area',Aws));
disp(sprintf('Aw=''%0.4d''cm^2 Selected area of a single strand',Aw));
disp(sprintf('PS=''%d''Number of primary strands',PS));
disp(sprintf('SS=''%d''Number of secondary strands',SS));
disp(sprintf('di=''%0.2d''mm Isolation distance between windings',dimin));
```

```matlab
disp(sprintf('Lkp=''%0.2d''H Leakage inductance',Lkp));
disp(sprintf('Vt=''%0.2d''dm^3 Total volume',Vtd));
disp(sprintf('Pcu=''%0.2d''W Winding loss',Pcu));
disp(sprintf('Pfe=''%0.2d''W Core loss',Pfei));
disp(sprintf('Effi=''%0.2d''Efficiency',Effi));
disp(sprintf('DT2=''%0.2d''C Temperature rise',DT2));
disp(' ')
disp('===== END =====')

%% REFERENCES

%[1]W. G. Hurley, W.H. Wölfle, Transformers and Inductors for Power
Electronics: Theory, Design and Applications, 1st ed., Wiley, 2013.

%[2]C. William, T. McLyman, Transformer and Inductor Design Handbook, 4th
ed., Taylor & Francis Group, 2011.

%[3]K. D. Hoang, J. Wang, "Design optimization of high-frequency transformer
for dual active bridge dc-dc converter,"
%Electrical Machines (ICEM), 2012 XXth International Conference, pp. 2311-
2317, Sept. 2012.

%[4]G. Ortiz, J. Biela, J. W. Kolar, "Optimized design of medium frequency
transformers with high isolation requirements,"
%in Proceeding of the 36th IEEE Industrial Electronics Society Conference,
IECON 2010, pp. 631-638, Nov. 2010.

%[5]"Estimating temperature rise of transformers," [Online]. Available:
%http://www.tscinternational.com/tech12.pdf [Accessed May 2015].
```

APPENDIX B.2

DESIGN EXAMPLES

This appendix presents the transformer design examples as obtained from the MATLAB®

program given in the Appendix B.1. These design examples are explained in Section 4.4.

Design Example #1: 200 kVA, 3 kHz, 3800/400 V, shell-type transformer

>> Thesis_HF_Transformer_Design_Algorithm_v2

===== HIGH-FREQUENCY TRANSFORMER DESIGN TOOL =====

WITH THIS TOOL YOU WILL BE DESIGNING A SINGLE-PHASE HIGH- OR MEDIUM-

FREQUENCY TRANSFORMER

SHELL-TYPE OR CORE-TYPE STRUCTURE

FOR MORE INFORMATION REFER TO THE THESIS:

 "HIGH-FREQUENCY TRANSFORMER DESIGN FOR SOLID-STATE TRANSFORMERS

IN ELECTRIC POWER DISTRIBUTION SYSTEMS"

BY RODERICK J. GARCIA M.

 To interrupt this program at any time enter "ctrl+c"

 ===== STEP 1. SYSTEM AND TOPOLOGY SPECIFICATIONS =====

 Enter output power (VA): 200e3

Enter expected efficiency (%): 98

Enter primary voltage (V): 3800

Enter secondary voltage (V): 400

Enter the isolation voltage level "Viso"(kV): 95

Enter primary current (A): 85

Enter secondary current (A): 807.5

Enter operating frequency (Hz): 3e3

Enter ambient temperature (C): 30

Enter expected temperature rise (C): 70

Enter duty cycle (between 0 and 1): 0.5

Enter waveform factor Kv (Ex. Square wave Kv=4 / Sinusoidal Kv=4.44): 4

Enter desired leakage inductance in (H): 3.01e-3

Enter window utilization factor (between 0 and 1)(Ex. 0.4): 0.4

===== STEP 2. MATERIAL PROPERTIES =====

Core Material

Enter selected core material: 1 for amorphous, 2 for ferrite, 3 for nanocrystalline, or 4 for other: 1

 Insulation Material

Enter dielectric strength of selected insulation material "Eins" in (kV/mm): 27

Enter a safety margin for isolation requirement "kiso"(Ex. 0.4): 0.4

===== STEP 3. OPTIMUM FLUX DENSITY =====

 Bop =

   0.2877

This is the calculated optimum flux density. Bear in mind the tradeoff between efficiency and volume.

If the flux density is increased, the volume can be reduced, but also the efficiency gets reduced

**Always consider Bop < Bsat

 If Bop is the desired flux density, enter Y, if this is not the desired flux density, enter N: n

Enter the desired flux density in (T): 0.3

===== STEP 4. CORE DIMENSIONS =====

 Area Product:

Ap =

  2.2976e+04

Based on Ap, select a core from a data sheet whose area product is larger than the calculated

value

Consider stacked cores if the larger area product in the data sheet is not sufficient

Enter the selected core series number (Ex. AMCC-100): AMCC-1000

Enter the number of stacked cores needed to achieve optimum Ap. If stacked cores are not

needed, enter 1: 24

If a Shell-type transformer structure is considered, enter "S" If a Core-type is considered, enter

"C": S

Now you have to enter the core dimensions from data sheet. See Metglas data sheet for label

references

Enter the total width "d"(cm): 8.5

Enter the height of the window area "c" (cm): 10.5

Enter height of the core "f" (cm): 17.1

Enter the length of the window area "b" (cm): 4

Enter the length of the core "e" (cm): 10.6

Enter the mean length of the core "lm" (cm): 42.7

Enter the cross sectional area of the core "Ac" (cm^2): 23

Enter the mass of the core (g): 7109

Enter the density of the core (g/cm^3): 7.18

This is the real area product of the core:

Ap =

    92736

===== STEP 5. WINDING CHARACTERIZATION =====

Calculated current density J (A/cm^2)

J =

  107.9851

Required total wire area based on current density, and primary and secondary currents (cm^2)

Awp =

  0.7871

Aws =

  7.4779

Skin depth (cm):

skin =

  0.1209

Maximum wire diameter (single strand) (cm):

dskin =

  0.2417

Maximum wire area (single strand) (cm^2):

Askin =

  0.0459

Enter area of selected strand size based on Askin or dskin (cm^2): 8.228e-3

Enter conductor resistivity @20 C(uOhm/cm): 209.5

Resistivity of the selected conductor at maximum operating temperature (uOhm/cm):

rhomax =

  275.3668

Minimum number of primary strands "PS"

PS =

  96

If PS is the desired number of primary strands, enter Y. If not, enter N: n

Enter the desired PS: 100

Minimum number of secondary strands "SS"

SS =

  909

If SS is the desired number of secondary strands, enter Y. If not, enter N: n

Enter the desired SS: 1000

Number of primary turns "Np":

Np =

  11

The number of turns is a free parameter that can adjust the leakage inductance

If Np is the desired number of primary turns, enter Y. If not, enter N: n

Enter the desired Np: 18

Number of secondary turns "Ns":

Ns =

  1.8947

If Ns is the desired number of secondary turns, enter Y. If not, enter N: n

Enter the desired Ns: 2

Mean Length Turn (MLT):

MLT =

 437.6531

Verify that the selected winding arrangement can actually fit in the core window area

===== STEP 6. ISOLATION DISTANCE =====

 This is the minimum isolation distance between primary and secondary windings based

on the isolation level and insulation material (mm):

dimin =

   8.7963

The isolation distance dimin could be increased in order to adjust the leakage inductance

**di>dimin

If dimin is the desired isolation distance, enter Y. If not, enter N: n

Enter the desired di: 35

 ===== STEP 7. LEAKAGE INDUCTANCE ESTIMATION =====

 This estimation is only applicable to a shell-type structure. If a Core-type structure was selected,

a leakage inductance estimation would require 2D or 3D Finite Element simulations

Calculated leakage inductance (H):

Lkp =

   0.0031

 ===== STEP 8. VOLUMEN CALCULATION =====

 Calculated volume of windings (cm^3)

Vw =

3.6763e+04

Calculated volume of core (cm^3)

Vc =

4.7141e+04

Calculated total volume (dm^3)

Vtd =

83.9037

===== STEP 9. LOSSES CALCULATION =====

 Core loss using the iGSE

in (W/m^3):

Pvi =

2.7182e+04

in (W):

Pfei =

2.2807e+03

Winding loss (W):

Pcu =

313.8952

Total loss (W):

Pt =

2.5946e+03

===== STEP 10. EFFICIENCY & TEMPERATURE RISE =====

Calculated efficiency:

Effi =

   0.9872

The efficiency could be increased in a second iteration by reducing the operating flux density in

Step 3.

If the optimum flux density has been used and the obtained efficiency is not desired, consider

using a different core material.

Temperature rise estimation:

Surface area (cm^2):

At =

   1.1937e+04

Estimated temperature rise (Celsius):

DT2 =

   88.4814

The calculated temperature rise exceeds the desired value previously entered

To continue with this temperature rise enter Y. To reject this and start the design process over

enter N: y

 ===== SUMMARY OF THE RESULTS =====

 Pout='200000'VA Rated power

Vp='3800'V Primary voltage

Vs='400'V Secondary voltage

f='3000'Hz Frequency

Core material = Amorphous

Core='AMCC-1000'Core number

B='3.00e-01'T Flux density

Np='18'Primary turns

Ns='2'Secondary turns

Awp='7.8715e-01'cm^2 Required total primary wire area

Aws='7.4779e+00'cm^2 Required total secondary wire area

Aw='8.2280e-03'cm^2 Selected area of a single strand

PS='100'Number of primary strands

SS='1000'Number of secondary strands

di='35'mm Isolation distance between windings

Lkp='3.12e-03'H Leakage inductance

Vt='8.39e+01'dm^3 Total volume

Pcu='3.14e+02'W Winding loss

Pfe='2.28e+03'W Core loss

Effi='9.87e-01'Efficiency

DT2='8.85e+01'C Temperature rise

 ===== END =====

Design Example #2: 20kVA, 3 kHz, 3800/400 V, core-type transformer

>> Thesis_HF_Transformer_Design_Algorithm_v2

===== HIGH-FREQUENCY TRANSFORMER DESIGN TOOL =====

WITH THIS TOOL YOU WILL BE DESIGNING A SINGLE-PHASE HIGH- OR MEDIUM-

FREQUENCY TRANSFORMER

SHELL-TYPE OR CORE-TYPE STRUCTURE

FOR MORE INFORMATION REFER TO THE THESIS:

 "HIGH-FREQUENCY TRANSFORMER DESIGN FOR SOLID-STATE TRANSFORMERS

IN ELECTRIC POWER DISTRIBUTION SYSTEMS"

BY RODERICK J. GARCIA M.

 To interrupt this program at any time enter "ctrl+c"

 ===== STEP 1. SYSTEM AND TOPOLOGY SPECIFICATIONS =====

 Enter output power (VA): 20e3

Enter expected efficiency (%): 98

Enter primary voltage (V): 3800

Enter secondary voltage (V): 400

Enter the isolation voltage level "Viso"(kV): 65

Enter primary current (A): 9

Enter secondary current (A): 82

Enter operating frequency (Hz): 3e3

Enter ambient temperature (C): 30

Enter expected temperature rise (C): 65

Enter duty cycle (between 0 and 1): 0.5

Enter waveform factor Kv (Ex. Square wave Kv=4 / Sinusoidal Kv=4.44): 4

Enter desired leakage inductance in (H): 60.2e-3

Enter window utilization factor (between 0 and 1)(Ex. 0.4): 0.4

===== STEP 2. MATERIAL PROPERTIES =====

Core Material

Enter selected core material: 1 for amorphous, 2 for ferrite, 3 for nanocrystalline, or 4 for other: 1

Insulation Material

Enter dielectric strength of selected insulation material "Eins" in (kV/mm): 27

Enter a safety margin for isolation requirement "kiso"(Ex. 0.4): 0.4

===== STEP 3. OPTIMUM FLUX DENSITY =====

Bop =

   0.4019

This is the calculated optimum flux density. Bear in mind the tradeoff between efficiency and volume.

If the flux density is increased, the volume can be reduced, but also the efficiency gets reduced

**Always consider Bop < Bsat

 If Bop is the desired flux density, enter Y, if this is not the desired flux density, enter N: y

===== STEP 4. CORE DIMENSIONS =====

 Area Product:

Ap =

   1.2349e+03

Based on Ap, select a core from a data sheet whose area product is larger than the calculated

value. Consider stacked cores if the larger area product in the data sheet is not sufficient

Enter the selected core series number (Ex. AMCC-100): AMCC-1000

Enter the number of stacked cores needed to achieve optimum Ap. If stacked cores are not

needed, enter 1: 2

If a Shell-type transformer structure is considered, enter "S" If a Core-type is considered, enter

"C": c

Now you have to enter the core dimensions from data sheet. See Metglas data sheet for label

references

Enter the total width "d" (cm): 8.5

Enter the height of the window area "c" (cm): 10.5

Enter height of the core "f" (cm): 17.1

Enter the length of the window area "b" (cm): 4

Enter the length of the core "e" (cm): 10.6

Enter the mean length of the core "lm" (cm): 42.7

Enter the cross sectional area of the core "Ac" (cm^2): 23

Enter the mass of the core (g): 7109

Enter the density of the core (g/cm^3): 7.18

This is the real area product of the core:

Ap =

    1932

===== STEP 5. WINDING CHARACTERIZATION =====

Calculated current density J (A/cm^2)

J =

  168.8210

Required total wire area based on current density, and primary and secondary currents (cm^2)

Awp =

  0.0533

Aws =

  0.4857

Skin depth (cm):

skin =

  0.1209

Maximum wire diameter (single strand) (cm):

dskin =

  0.2417

Maximum wire area (single strand) (cm^2):

Askin =

  0.0459

Enter area of selected strand size based on Askin or dskin (cm^2): 0.5067e-3

Enter conductor resistivity @20 C(uOhm/cm): 3402

Resistivity of the selected conductor at maximum operating temperature (uOhm/cm):

rhomax =

  4.4047e+03

Minimum number of primary strands "PS"

PS =

  105

If PS is the desired number of primary strands, enter Y. If not, enter N: n

Enter the desired PS: 110

Minimum number of secondary strands "SS"

SS =

   959

If SS is the desired number of secondary strands, enter Y. If not, enter N: n

Enter the desired SS: 1100

Number of primary turns "Np":

Np =

   181

The number of turns is a free parameter that can adjust the leakage inductance

If Np is the desired number of primary turns, enter Y. If not, enter N: y

Number of secondary turns "Ns":

Ns =

   19.0526

If Ns is the desired number of secondary turns, enter Y. If not, enter N: n

Enter the desired Ns: 20

Mean Length Turn (MLT):

MLT =

   57.0531

Verify that the selected winding arrangement can actually fit in the core window area

===== STEP 6. ISOLATION DISTANCE =====

This is the minimum isolation distance between primary and secondary windings based

on the isolation level and insulation material (mm):

dimin =

  6.0185

The isolation distance dimin could be increased in order to adjust the leakage inductance

**di>dimin

If dimin is the desired isolation distance, enter Y. If not, enter N: n

Enter the desired di: 8

===== STEP 7. LEAKAGE INDUCTANCE ESTIMATION =====

This estimation is only applicable to a shell-type structure. If a Core-type structure was selected,

a leakage inductance estimation would require 2D or 3D Finite Element simulations

Calculated leakage inductance (H):

Lkp =

  0.0252

The estimated leakage inductance is lower than the desired value previously entered

To continue with this leakage inductance enter Y. To reject this design and start over enter N: y

===== STEP 8. VOLUMEN CALCULATION =====

Calculated volume of windings (cm^3)

Vw =

  2.3962e+03

Calculated volume of core (cm^3)

Vc =

  1.9642e+03

Calculated total volume (dm^3)

Vtd =

4.3604

===== STEP 9. LOSSES CALCULATION =====

Core loss using the iGSE

in (W/m^3):

Pvi =

  4.5220e+04

in (W):

Pfei =

  197.1778

Winding loss (W):

Pcu =

  64.2173

Total loss (W):

Pt =

  261.3951

===== STEP 10. EFFICIENCY & TEMPERATURE RISE =====

Calculated efficiency:

Effi =

  0.9871

The efficiency could be increased in a second iteration by reducing the operating flux density in

Step 3.

If the optimum flux density has been used and the obtained efficiency is not desired, consider

using a different core material.

Temperature rise estimation:

Surface area (cm^2):

At =

 1.7230e+03

Estimated temperature rise (Celsius):

DT2 =

 65.5812

The calculated temperature rise exceeds the desired value previously entered

To continue with this temperature rise enter Y. To reject this and start the design process over

enter N: y

===== SUMMARY OF THE RESULTS =====

Pout='20000'VA Rated power

Vp='3800'V Primary voltage

Vs='400'V Secondary voltage

f='3000'Hz Frequency

Core material = Amorphous

Core='AMCC-1000'Core number

B='4.02e-01'T Flux density

Np='181'Primary turns

Ns='20'Secondary turns

Awp='5.3311e-02'cm^2 Required total primary wire area

Aws='4.8572e-01'cm^2 Required total secondary wire area

Aw='5.0670e-04'cm^2 Selected area of a single strand

PS='110'Number of primary strands

SS='1100'Number of secondary strands

di='08'mm Isolation distance between windings

Lkp='2.52e-02'H Leakage inductance

Vt='4.36e+00'dm^3 Total volume

Pcu='6.42e+01'W Winding loss

Pfe='1.97e+02'W Core loss

Effi='9.87e-01'Efficiency

DT2='6.56e+01'C Temperature rise

===== END =====

Design Example #3: 2 kVA, 20 kHz, 600/60 V, shell-type transformer

>> Thesis_HF_Transformer_Design_Algorithm_v2

===== HIGH-FREQUENCY TRANSFORMER DESIGN TOOL =====

WITH THIS TOOL YOU WILL BE DESIGNING A SINGLE-PHASE HIGH- OR MEDIUM-

FREQUENCY TRANSFORMER

SHELL-TYPE OR CORE-TYPE STRUCTURE

FOR MORE INFORMATION REFER TO THE THESIS:

 "HIGH-FREQUENCY TRANSFORMER DESIGN FOR SOLID-STATE TRANSFORMERS

IN ELECTRIC POWER DISTRIBUTION SYSTEMS"

BY RODERICK J. GARCIA M.

 To interrupt this program at any time enter "ctrl+c"

 ===== STEP 1. SYSTEM AND TOPOLOGY SPECIFICATIONS =====

 Enter output power (VA): 2e3

Enter expected efficiency (%): 98

Enter primary voltage (V): 600

Enter secondary voltage (V): 60

Enter the isolation voltage level "Viso"(kV): 1

Enter primary current (A): 4

Enter secondary current (A): 40

Enter operating frequency (Hz): 20e3

Enter ambient temperature (C): 25

Enter expected temperature rise (C): 60

Enter duty cycle (between 0 and 1): 0.5

Enter waveform factor Kv (Ex. Square wave Kv=4 / Sinusoidal Kv=4.44): 4

Enter desired leakage inductance in (H): 1.1e-3

Enter window utilization factor (between 0 and 1)(Ex. 0.4): 0.4

===== STEP 2. MATERIAL PROPERTIES =====

 Core Material

Enter selected core material: 1 for amorphous, 2 for ferrite, 3 for nanocrystalline, or 4 for other: 1

 Insulation Material

Enter dielectric strength of selected insulation material "Eins" in (kV/mm): 15

Enter a safety margin for isolation requirement "kiso"(Ex. 0.4): 0.4

===== STEP 3. OPTIMUM FLUX DENSITY =====

 Bop =

   0.1443

This is the calculated optimum flux density. Bear in mind the tradeoff between efficiency and

volume.

If the flux density is increased, the volume can be reduced, but also the efficiency gets reduced

**Always consider Bop < Bsat

 If Bop is the desired flux density, enter Y, if this is not the desired flux density, enter N: n

Enter the desired flux density in (T): 0.15

===== STEP 4. CORE DIMENSIONS =====

 Area Product:

Ap =

  32.8275

Based on Ap, select a core from a data sheet whose area product is larger than the calculated value. Consider stacked cores if the larger area product in the data sheet is not sufficient

 Enter the selected core series number (Ex. AMCC-100): AMCC-50

Enter the number of stacked cores needed to achieve optimum Ap. If stacked cores are not needed, enter 1: 1

If a Shell-type transformer structure is considered, enter "S" If a Core-type is considered, enter "C": S

Now you have to enter the core dimensions from data sheet. See Metglas data sheet for label references

Enter the total width "d" (cm): 2.5

Enter the height of the window area "c" (cm): 7

Enter height of the core "f" (cm): 10.2

Enter the length of the window area "b" (cm): 2

Enter the length of the core "e" (cm): 5.2

Enter the mean length of the core "lm" (cm): 24.9

Enter the cross sectional area of the core "Ac" (cm^2): 3.3

Enter the mass of the core (g): 586

Enter the density of the core (g/cm^3): 7.18

This is the real area product of the core:

Ap =

 184.8000

===== STEP 5. WINDING CHARACTERIZATION =====

Calculated current density J (A/cm^2)

J =

217.4997

Required total wire area based on current density, and primary and secondary currents (cm^2)

Awp =

0.0184

Aws =

0.1839

Skin depth (cm):

skin =

0.0468

Maximum wire diameter (single strand) (cm):

dskin =

0.0936

Maximum wire area (single strand) (cm^2):

Askin =

0.0069

Enter area of selected strand size based on Askin or dskin (cm^2): 0.1266e-3

Enter conductor resistivity @20 C(uOhm/cm): 13608

Resistivity of the selected conductor at maximum operating temperature (uOhm/cm):

rhomax =

1.7084e+04

Minimum number of primary strands "PS"

PS =

145

If PS is the desired number of primary strands, enter Y. If not, enter N: n

Enter the desired PS: 259

Minimum number of secondary strands "SS"

SS =

    1453

If SS is the desired number of secondary strands, enter Y. If not, enter N: n

Enter the desired SS: 1554

Number of primary turns "Np":

Np =

  80

The number of turns is a free parameter that can adjust the leakage inductance

If Np is the desired number of primary turns, enter Y. If not, enter N: y

Number of secondary turns "Ns":

Ns =

  8

If Ns is the desired number of secondary turns, enter Y. If not, enter N: y

Mean Length Turn (MLT):

MLT =

  19.6265

Verify that the selected winding arrangement can actually fit in the core window area

===== STEP 6. ISOLATION DISTANCE =====

 This is the minimum isolation distance between primary and secondary windings based

on the isolation level and insulation material (mm):

dimin =

   0.1667

The isolation distance dimin could be increased in order to adjust the leakage inductance

**di>dimin

If dimin is the desired isolation distance, enter Y. If not, enter N: n

Enter the desired di: 0.2

===== STEP 7. LEAKAGE INDUCTANCE ESTIMATION =====

This estimation is only applicable to a shell-type structure. If a Core-type structure was selected,

a leakage inductance estimation would require 2D or 3D Finite Element simulations

Calculated leakage inductance (H):

Lkp =

   0.0019

===== STEP 8. VOLUMEN CALCULATION =====

 Calculated volume of windings (cm^3)

Vw =

  549.5434

Calculated volume of core (cm^3)

Vc =

  164.3400

Calculated total volume (dm^3)

Vtd =

   0.7139

===== STEP 9. LOSSES CALCULATION =====

Core loss using the iGSE

in (W/m^3):

Pvi =

  1.4276e+05

in (W):

Pfei =

  101.9113

Winding loss (W):

Pcu =

  4.4189

Total loss (W):

Pt =

  106.3302

===== STEP 10. EFFICIENCY & TEMPERATURE RISE =====

Calculated efficiency:

Effi =

  0.9495

The efficiency could be increased in a second iteration by reducing the operating flux density in

Step 3.

If the optimum flux density has been used and the obtained efficiency is not desired, consider

using a different core material.

Temperature rise estimation:

Surface area (cm^2):

At =

  532.8894

Estimated temperature rise (C):

DT2 =

  82.3979

The calculated temperature rise exceeds the desired value previously entered

To continue with this temperature rise enter Y. To reject this and start the design process over

enter N: y

 ===== SUMMARY OF THE RESULTS =====

 Pout='2000'VA Rated power

Vp='600'V Primary voltage

Vs='60'V Secondary voltage

f='20000'Hz Frequency

Core material = Amorphous

Core='AMCC-50'Core number

B='1.50e-01'T Flux density

Np='80'Primary turns

Ns='8'Secondary turns

Awp='1.8391e-02'cm^2 Required total primary wire area

Aws='1.8391e-01'cm^2 Required total secondary wire area

Aw='1.2660e-04'cm^2 Selected area of a single strand

PS='259'Number of primary strands

SS='1554'Number of secondary strands

di='2.00e-01'mm Isolation distance between windings

Lkp='1.86e-03'H Leakage inductance

Vt='7.14e-01'dm^3 Total volume

Pcu='4.42e+00'W Winding loss

Pfe='1.02e+02'W Core loss

Effi='9.50e-01'Efficiency

DT2='8.24e+01'C Temperature rise

 ===== END =====

Design Example #4: 2 kVA, 3 kHz, 600/60 V, core-type transformer

>> Thesis_HF_Transformer_Design_Algorithm_v2

===== HIGH-FREQUENCY TRANSFORMER DESIGN TOOL =====

WITH THIS TOOL YOU WILL BE DESIGNING A SINGLE-PHASE HIGH- OR MEDIUM-

FREQUENCY TRANSFORMER

SHELL-TYPE OR CORE-TYPE STRUCTURE

FOR MORE INFORMATION REFER TO THE THESIS:

 "HIGH-FREQUENCY TRANSFORMER DESIGN FOR SOLID-STATE TRANSFORMERS

IN ELECTRIC POWER DISTRIBUTION SYSTEMS"

BY RODERICK J. GARCIA M.

 To interrupt this program at any time enter "ctrl+c"

 ===== STEP 1. SYSTEM AND TOPOLOGY SPECIFICATIONS =====

 Enter output power (VA): 2e3

Enter expected efficiency (%): 98

Enter primary voltage (V): 600

Enter secondary voltage (V): 60

Enter the isolation voltage level "Viso"(kV): 1

Enter primary current (A): 4

Enter secondary current (A): 40

Enter operating frequency (Hz): 20e3

Enter ambient temperature (C): 25

Enter expected temperature rise (C): 60

Enter duty cycle (between 0 and 1): 0.5

Enter waveform factor Kv (Ex. Square wave Kv=4 / Sinusoidal Kv=4.44): 4

Enter desired leakage inductance in (H): 1.1e-3

Enter window utilization factor (between 0 and 1)(Ex. 0.4): 0.4

===== STEP 2. MATERIAL PROPERTIES =====

 Core Material

Enter selected core material: 1 for amorphous, 2 for ferrite, 3 for nanocrystalline, or 4 for other: 1

 Insulation Material

Enter dielectric strength of selected insulation material "Eins" in (kV/mm): 15

Enter a safety margin for isolation requirement "kiso"(Ex. 0.4): 0.4

===== STEP 3. OPTIMUM FLUX DENSITY =====

Bop =

    0.1443

This is the calculated optimum flux density. Bear in mind the tradeoff between efficiency and

volume.

If the flux density is increased, the volume can be reduced, but also the efficiency gets reduced

**Always consider Bop < Bsat

 If Bop is the desired flux density, enter Y, if this is not the desired flux density, enter N: n

Enter the desired flux density in (T): 0.15

===== STEP 4. CORE DIMENSIONS =====

 Area Product:

Ap =

  32.8275

Based on Ap, select a core from a data sheet whose area product is larger than the calculated

value. Consider stacked cores if the larger area product in the data sheet is not sufficient

 Enter the selected core series number (Ex. AMCC-100): AMCC-80

Enter the number of stacked cores needed to achieve optimum Ap. If stacked cores are not

needed, enter 1: 1

If a Shell-type transformer structure is considered, enter "S" If a Core-type is considered, enter

"C": C

Now you have to enter the core dimensions from data sheet. See Metglas data sheet for label

references

Enter the total width "d" (cm): 4

Enter the height of the window area "c" (cm): 7

Enter height of the core "f" (cm): 10.2

Enter the length of the window area "b" (cm): 2

Enter the length of the core "e" (cm): 5.2

Enter the mean length of the core "lm" (cm): 25.4

Enter the cross sectional area of the core "Ac" (cm^2): 5.2

Enter the mass of the core (g): 938

Enter the density of the core (g/cm^3): 7.18

This is the real area product of the core:

Ap =

  72.8000

===== STEP 5. WINDING CHARACTERIZATION =====

Calculated current density J (A/cm^2)

J =

  244.3599

Required total wire area based on current density, and primary and secondary currents (cm^2)

Awp =

  0.0164

Aws =

  0.1637

Skin depth (cm):

skin =

  0.0468

Maximum wire diameter (single strand) (cm):

dskin =

  0.0936

Maximum wire area (single strand) (cm^2):

Askin =

  0.0069

Enter area of selected strand size based on Askin or dskin (cm^2): 0.1266e-3

Enter conductor resistivity @20 C(uOhm/cm): 13608

Resistivity of the selected conductor at maximum operating temperature (uOhm/cm):

rhomax =

  1.7084e+04

Minimum number of primary strands "PS"

PS =

  129

If PS is the desired number of primary strands, enter Y. If not, enter N: n

Enter the desired PS: 259

Minimum number of secondary strands "SS"

SS =

   1293

If SS is the desired number of secondary strands, enter Y. If not, enter N: n

Enter the desired SS: 1554

Number of primary turns "Np":

Np =

  102

The number of turns is a free parameter that can adjust the leakage inductance

If Np is the desired number of primary turns, enter Y. If not, enter N: n

Enter the desired Np: 100

Number of secondary turns "Ns":

Ns =

  10

If Ns is the desired number of secondary turns, enter Y. If not, enter N: y

Mean Length Turn (MLT):

MLT =

  19.4265

Verify that the selected winding arrangement can actually fit in the core window area

===== STEP 6. ISOLATION DISTANCE =====

 This is the minimum isolation distance between primary and secondary windings based

on the isolation level and insulation material (mm):

dimin =

   0.1667

The isolation distance dimin could be increased in order to adjust the leakage inductance

**di>dimin

If dimin is the desired isolation distance, enter Y. If not, enter N: n

Enter the desired di: 0.2

 ===== STEP 7. LEAKAGE INDUCTANCE ESTIMATION =====

 This estimation is only applicable to a shell-type structure. If a Core-type structure was selected,

a leakage inductance estimation would require 2D or 3D Finite Element simulations

Calculated leakage inductance (H):

Lkp =

   0.0029

 ===== STEP 8. VOLUMEN CALCULATION =====

 Calculated volume of windings (cm^3)

Vw =

  271.9717

Calculated volume of core (cm^3)

Vc =

  132.0800

Calculated total volume (dm^3)

Vtd =

  0.4041

===== STEP 9. LOSSES CALCULATION =====

 Core loss using the iGSE

in (W/m^3):

Pvi =

  1.4276e+05

in (W):

Pfei =

  57.6809

Winding loss (W):

Pcu =

  5.4674

Total loss (W):

Pt =

  63.1482

===== STEP 10. EFFICIENCY & TEMPERATURE RISE =====

Calculated efficiency:

Effi =

  0.9694

The efficiency could be increased in a second iteration by reducing the operating flux density in

Step 3.

If the optimum flux density has been used and the obtained efficiency is not desired, consider using a different core material.

Temperature rise estimation:

Surface area (cm^2):

At =

  334.4658

Estimated temperature rise (C):

DT2 =

  78.6893

The calculated temperature rise exceeds the desired value previously entered

To continue with this temperature rise enter Y. To reject this and start the design process over enter N: y

 ===== SUMMARY OF THE RESULTS =====

 Pout='2000'VA Rated power

Vp='600'V Primary voltage

Vs='60'V Secondary voltage

f='20000'Hz Frequency

Core material = Amorphous

Core='AMCC-80'Core number

B='1.50e-01'T Flux density

Np='100'Primary turns

Ns='10'Secondary turns

Awp='1.6369e-02'cm^2 Required total primary wire area

Aws='1.6369e-01'cm^2 Required total secondary wire area

Aw='1.2660e-04'cm^2 Selected area of a single strand

PS='259'Number of primary strands

SS='1554'Number of secondary strands

di='2.00e-01'mm Isolation distance between windings

Lkp='2.87e-03'H Leakage inductance

Vt='4.04e-01'dm^3 Total volume

Pcu='5.47e+00'W Winding loss

Pfe='5.77e+01'W Core loss

Effi='9.69e-01'Efficiency

DT2='7.87e+01'C Temperature rise

 ===== END =====

CHAPTER 5

CONCLUSIONS AND RECOMMENDATIONS FOR FUTURE WORK

5.1 Conclusions

The availability of functionalities such as power flow control, voltage regulation, harmonic suppression, voltage sag ride through capability, and volume and weight reductions make the SST an enabling technology for future energy systems and applications characterized by space limitations [1], [2]. However, the design of the HF/MF transformer, one of the main components in a SST, must be carefully considered especially in high-voltage high-power applications because of the current and voltage requirements imposed by the different SST topologies, the increment in losses, the effects due to the high-frequency operation, and the isolation requirements [3], [4].

In Chapter 2, different topologies to realize a SST were presented and it was concluded that the main desired characteristics on a SST topology are: availability of a LV DC link, modularity capability, unidirectional or bidirectional power flow control functionality, reduced number of components, and soft switching operation. Therefore, topologies consisting of two or three stages with a LV DC link are the most suitable for the SST implementation since they can provide the main features desired in future energy systems [5], [6]. This explains why topologies consisting of an active-front-end rectifier stage (AC-DC), a DC to DC stage with a HF or MF transformer, and a back-end inverter stage (DC-AC) have been proposed the most for SST applications and considered for the selected case study.

In particular, three SST topologies were selected to analyze the case study. Topology (I) which consists of full bridges on HV and LV side, topology (II) with half bridges on HV side and full bridges on LV side, and topology (III) with half bridges on HV and LV side. It was observed

that different topologies can lead to different current and voltage stresses on the HF/MF transformer which has an impact on the isolation requirements. For instance, the voltage stress on the transformer for topology (I) was 3.8 kV; while for topology (II) and (III) was 1.9 kV for the same power rating. However, the HF transformer should be in compliance with international standards for distribution transformers. For example, considering the isolation requirement, an isolation level of 95 kV should be considered for the case study.

In addition, each topology resulted in different leakage inductance requirements for maximum power transfer in the DC-DC converter stage. The leakage inductance for topology (I) was 3.01 mH; while for topology (II) and (III) were 0.63 mH and 0.71 mH, respectively. Therefore, it is suggested that the transformer design includes a leakage inductance specification in order to avoid the use of an additional inductor to meet the required inductance which could lead to a lower power density [7].

Effective techniques to adjust the transformer leakage inductance within the transformer design were explained in Chapter 3. The proposed design methodology uses as free parameters the number of turns in the windings and the isolation distance between the windings to adjust the desired inductance. These techniques can be easily implemented in a design software to be used as a tool. Other techniques to adjust the leakage inductance are to change the transformer structure (e.g., core-type or shell-type structure), or insert a layer of a magnetic material with high permeability between the windings to increase the leakage inductance [8].

In Chapter 3, four design considerations were investigated in order to stablish the basics for the proposed HF/MF transformer design:

- Core material selection
- HF effects in core and windings

- Isolation requirement

- Leakage inductance integration

On the core material selection, a magnetic core characterization was presented considering four magnetic materials: ferrite, silicon steel, amorphous, and nanocrystalline. Due to the low saturation flux density of the ferrite and the high manufacturing cost of the nanocrystalline material, they are not recommended for the considered application. Therefore, amorphous material that presents high saturation flux density and relatively low core-loss density, and silicon steel with thin laminations to minimize eddy current losses are the most suitable for distribution applications [9].

A review of the main core loss calculation methods that have been proposed in the literature for nonsinusoidal excitations was also presented in Chapter 3. One of the most recent methods is the i^{2}GSE proposed in [10] which considers the relaxation effects in the magnetic material during zero-voltage conditions; thus, it is more accurate for low duty cycles (D < 0.2) compared with the iGSE. The inaccuracies of the iGSE for low duty cycles were validated with experimental results presented in Appendix A.1 where the two-winding method was selected for the core loss measurements [11].

The HF effects in the windings (i.e., skin and proximity effects) are taken care of by using the so-called Litz wire for the windings. In addition, the isolation requirement can be considered within the transformer design by calculating a minimum isolation distance between windings [12]. The resulting isolation distance for the case study considering a BIL of 95 kV was 16 mm. This distance can also be used as a free parameter to adjust the transformer leakage inductance according to the required value for maximum power transfer [12].

These design considerations were integrated into the proposed transformer design methodology presented in Chapter 4 that has been implemented in MATLAB® as an interactive tool for designing HF/MF transformers. The design tool is applicable to single-phase HF/MF transformers with either core-type or shell-type structures. The flux density optimization procedure presented in [13] is adopted in order to maximize transformer's efficiency. Furthermore, the design methodology accounts for the leakage inductance and isolation requirements.

5.2 Recommendations for Future Work

The work presented in this thesis could be extended per the following recommendations:

- Evaluate other SST topologies and their impact upon the transformer design in order to find the most suitable topology in terms of efficiency, functionalities, cost, and power density for a particular application.

- Amorphous and nanocrystalline materials seem to be the best candidates for SST applications due to their advantageous properties, as discussed in Chapter 3; however, new core magnetic materials (e.g. silicon steel with thin laminations) could be evaluated in order to be used in high-power applications (> 5MW) [9].

- The realization of SSTs with a three-phase arrangement has advantages over the single-phase arrangement in high-power applications, such as a smaller transformer area product, lower rms currents through the DC link capacitors, and lower turn-off switching loss [14]. Therefore, the HF/MF transformer design tool presented in Chapter 4 could be extended to account for the design of three-phase HF/MF transformers.

5.3 References

[1]   X. She, R. Burgos, G. Wang, F. Wang, A.Q. Huang, "Review of solid state transformer in the distribution system: From components to field application," in *Proceedings of the IEEE Energy Conversion Congress and Exposition*, ECCE 2012, pp. 4077–4084, Sept., 2012.

[2]   J. W. Kolar, G. Ortiz, "Solid-state-transformers: Key components of future traction and smart grid systems," in *Proceedings of the International Power Electronics Conference*, IPEC 2014, Japan, May 18-24, 2014.

[3]   G. Ortiz, J. Biela, J. W. Kolar, "Optimized design of medium frequency transformers with high isolation requirements," in *Proceedings of the 36th IEEE Industrial Electronics Society Conference*, IECON 2010, pp. 631-638, November 2010.

[4]   G. Ortiz, M. Leibl, J.W. Kolar, O. Apeldoorn, "Medium frequency transformers for solid-state-transformer applications — Design and experimental verification," in *Proceedings of the 10th IEEE International Conference on Power Electronics and Drive Systems*, PEDS 2013, pp. 1285–1290, April 2013.

[5]   S. Falcones, X. Mao, R. Ayyanar, "Topology Comparison for Solid State Transformer Implementation," *IEEE Power and Energy Society General Meeting*, pp. 1-8, Jul. 2010.

[6]   T. Zhao, "Design and control of a cascaded h-bridge converter based solid state transformer (SST)," Ph.D. dissertation, Dept. Elect. Eng., North Carolina State Univ., Raleigh, North Carolina, USA, 2010.

[7]   Y. Du, S. Baek, S. Bhattacharya, A. Q. Huang, "High-voltage high-frequency transformer design for a 7.2kV to 120V/240V 20kVA solid state transformer," in *Proceedings of the 36th Annual Conference on IEEE Industrial Electronics Society*, IECON 2010, pp. 493-498, Nov. 2010.

[8]   B. Cougo, J. W. Kolar, "Integration of Leakage Inductance in Tape Wound Core Transformers for Dual Active Bridge Converters," in *Proceedings of the 7th International Conference Integrated Power Electronics Systems* (CIPS), 2012, pp. 1-6, March 2012.

[9]   N. Soultau, H. Stagge, R. W. De Doncker, O. Apeldoorn, "Development and demonstration of a medium-voltage high-power DC-DC converter for DC distribution systems," in *Proceedings of the 5th IEEE International Symposium on Power Electronics for Distributed Generation Systems*, PEDG 2014, pp. 1-8, June 2014.

[10] J. Mühlethaler, J. Biela, J.W. Kolar, A. Ecklebe, "Improved core-loss calculation for magnetic components employed in power electronic systems," *IEEE Transactions on Power Electronics*, vol. 27, no. 2, pp. 964–973, February, 2012.

[11] R. Garcia, A. Escobar-Mejia, K. George, J.C. Balda, "Loss comparison of selected core magnetic materials operating at medium and high frequencies and different excitation voltages," in *Proceedings of the Power Electronics for Distributed Generation Systems*, PEDG 2014, pp. 1-6, June 2014.

[12] G. Ortiz, J. Biela, J. W. Kolar, "Optimized design of medium frequency transformers with high isolation requirements," in *Proceeding of the 36th IEEE Industrial Electronics Society Conference*, IECON 2010, pp. 631-638, Nov. 2010.

[13] W.G. Hurley, W. H. Wöfle, J. G. Breslin, "Optimized transformer design: Inclusive of high-frequency effects," *IEEE Transactions on Power Electronics*, vol. 13, no. 4, pp. 651-659, July 1998.

[14] R.W.A.A. De Doncker, D.M. Divan, M.H. Kheraluwala, "A three-phase soft-switched high-power-density DC/DC converter for high-power applications," *IEEE Transactions on Industry Applications*, vol. 27, no. 1, pp. 63-73, Jan./Feb. 1991.